

Supplementary Information

A STAT5B-CD9 axis determines self-renewal in hematopoietic and leukemic stem cells

This file includes the Supplementary Methods, Supplementary Tables S1 and S2, Supplementary Figures S1-S7, Supplementary Figure Legends, the Supplementary References and an Annex Part I (cropped western blot membranes with all loading controls) and Part II (uncropped western blot membranes). Supplementary Table S3 is provided as separate .xlsx file.

11 **Supplementary Materials and Methods**

12 *Graphical abstract*

13 The graphical abstract was created with BioRender.com.

14 *Primary patient-derived samples*

15 Primary patient BM samples (routine examinations at diagnosis) were obtained from 6 patients with
16 chronic phase CML, 8 with *FLT3*-ITD-mutated AML, 4 with *JAK2*^{V617F}-mutated MPN and one with a
17 *JAK2*^{V617F+} myelodysplastic/myeloproliferative (MDS/MPN) overlap syndrome (listed in
18 Supplementary **Table S2**). BM MNC were isolated using Ficoll and frozen.

19 *Cell culture maintenance*

20 HPC^{LSK} cells were generated, cultured and maintained as described¹. HPC-7 cells were maintained as
21 described². HEL, SET2 and K562 were cultured in RPMI medium supplemented with 10% heat-
22 inactivated fetal bovine serum (FBS), 50 μ M 2-mercaptoethanol, 100 U/ml penicillin, and 100 μ g/ml
23 streptomycin. Platinum-E (plat-E) cells were cultured and maintained in DMEM medium supplemented
24 with 10% FBS and 100 U/ml penicillin, and 100 μ g/ml streptomycin.

25 *Retroviral transductions*

26 Virus supernatants were produced using plat-E cells that were separately transfected with a pMSCV
27 retroviral vector containing following oncogenes: *JAK2*^{V617F}-GFP or *FLT3*-ITD-GFP using Turbofect
28 according to the manufacturer's instruction. BCR/ABL^{p210}-GFP virus was produced by gP^{p210}
29 BCR/ABL^{p210} retroviral producer cell line³. One day after transfection, medium was changed to IMDM
30 culture media of target cells. Viral supernatants were harvested, filtered (0.45 μ m), supplemented with
31 4 μ g/mL polybrene and 2% stem cell factor (SCF) for HPC-7 cells, 4 μ g/mL polybrene, 2% SCF and
32 12.5 ng/ml IL-6 for HPC^{LSK} cells, 4 μ g/mL polybrene, 2% SCF, 12.5 ng/ml IL-6, 10 ng/ml IL-3 and 25
33 ng/ml TPO for *ex vivo* FACS-sorted LSK cells. Target cells were infected with virus supernatant on
34 each of the following two days and GFP⁺ cells were FACS-sorted.

35 *Flow Cytometry*

36 Murine BM cells were recovered by crushing of femora and tibiae in PBS using a mortar and pestle.
37 The cell suspension was filtered through a 70 μ m cell strainer and washed once in PBS. Cells were
38 stained on ice for 45 min in 2% FBS/PBS.

39 For characterization of the HSC compartment and FACS-sorting of LSK or HSC/MPP1 cells derived
40 from BM of wt, *Stat5a*^{-/-}, *Stat5b*^{-/-}, cS5A^{hi} or STAT5B^{N642H} mice antibodies directed against Gr-1-
41 APC/Cy7, TER-119-APC/Cy7, CD19-APC/Cy7, CD3-APC/Cy7, Mac1-APC/Cy7, Sca1-PE/Cy7, c-
42 Kit-PE-Cy5, CD150-APC, CD48-PE, CD135-Biotin., CD34-FITC and Streptavidin-PB were used.

43 To detect CD9 levels on wt, *Stat5a*^{-/-}, *Stat5b*^{-/-}, cS5A^{hi}, STAT5B^{N642H} and *JAK2*^{V617F} LSK cells, BM cells
44 were stained with antibodies directed against: Gr-1-APC/Cy7, TER-119-APC/Cy7, CD19-APC/Cy7,
45 CD3-APC/Cy7, Mac1-APC/Cy7, Sca1-PE/Cy7, c-Kit-PE-Cy5 and CD9-PB.

46 For characterization of aCD9 blocking JAK2^{V617F} BM transplantation assays antibodies directed against
47 Gr-1-APC/Cy7, TER-119-APC/Cy7, CD19-APC/Cy7, CD3-APC/Cy7, Mac1-APC/Cy7, Sca1-PE/Cy7,
48 c-Kit-PE-Cy5, CD150-APC, CD48-PE, CD41-PB, Ly5.1-PE, Ly5.2-FITC, CD93-APC, CD43-Biotin,
49 Streptavidin-BV650, CD127-PB, CD19-BV605, Ly5.1-FITC, Ly5.2-PB were used.

50 For intracellular stainings the following antibodies were used: HSC/LSK: CD19-PB, CD11b-PB, Gr-1-
51 PB, TER-119-PB, CD3-PB, CD117-FITC, CD150-BV510, CD48-PE, LY-6A/E-Biotin., Streptavidin-
52 PE/Cy7; B-cells: CD45R-PE; T-cells: CD3-FITC; Granulocytes: Gr-1-FITC, CD11b-PE/Cy7; erythroid
53 cells: CD71-FITC; megakaryocytes: CD41-Biotin., Streptavidin-PE/Cy7; human patient BM MNC
54 samples: CD9-FITC; phospho-STAT5-APC, IgG-APC, STAT5.

55 Human patient samples were surface stained with antibodies against: CD34-PE, CD38-PE/Cy7, CD11b-
56 APC/Cy7, CD45-PB, CD9-FITC.

57 Samples were acquired using a FACS CantoII (BD), a Cytotflex (Beckman Coulter) or Cytotflex S
58 (Beckman Coulter) flow cytometer. Data were analysed using FACSDiva, CytExpert or FlowJo for data
59 analysis.

60 All high-purity FACS-sorting experiments were performed at 4 °C on a FACSAriaIII device equipped
61 with a 488 nm, 561 nm, 633 nm and 395 nm laser and analysed using FACSDiva software.

62 *Cell cycle staining*

63 KI67/DAPI staining was performed as previously described⁴. Cells were stained using antibodies
64 directed against: Gr-1-APC/Cy7, TER-119-APC/Cy7, CD19-APC/Cy7, CD3-APC/Cy7, Mac1-
65 APC/Cy7, Sca1-PE/Cy7, c-Kit-PE-Cy5, CD150-APC and CD48-PE, KI67 and 2 µg/ml DAPI.

66 *Apoptosis staining*

67 Cells were harvested and stained using antibodies directed against: Gr-1-APC/Cy7, TER-119-APC/Cy7,
68 CD19-APC/Cy7, CD3-APC/Cy7, Mac1-APC/Cy7, Sca1-PE/Cy7, c-Kit-PE-Cy5, CD150-APC and
69 CD48-PE. All further steps were performed in Annexin-V Binding Buffer (1x). Cells were washed and
70 incubated for 10-15 min at room temperature (RT) with KI67 antibody. After washing, cells were
71 resuspended in Annexin-V Binding Buffer containing 2 µg/ml DAPI.

72 *Intracellular staining*

73 For intracellular pYSTAT5 and STAT5 stainings several settings were used: 3x10⁶ BM cells of wt,
74 *Stat5a*^{-/-} or *Stat5b*^{-/-} mice were stimulated with: 100 ng/ml TPO (PeproTech 135-14) for CD150⁺CD48⁻
75 LSKs, 200 U/ml IL-2 and 50 ng/ml IL-7 for B-cells/T-cells, 100 ng/ml GM-CSF for
76 granulocytes/macrophages/neutrophils or 10 U/ml EPO for erythroid cells or 100 ng/ml TPO for
77 megakaryocytes. Cells were washed once in PBS and stained for surface markers CD150⁺CD48⁻LSK
78 cells or B-cells/T-cells (B220⁺/CD3⁺) or granulocytes/neutrophils (Gr-1⁺/CD11b⁺) or erythrocytes
79 (CD71⁺) or megakaryocytes (CD41⁺) OR 3x10⁶ BM cells of wt, cS5A^{hi} or STAT5B^{N642H} mice were
80 analysed *ex vivo* without cytokine stimulation. Cells were washed once in PBS and surface-stained for
81 CD150⁺CD48⁻LSK cells. OR 2.5x10⁵ AML^{FLT3-ITD⁺} patient BM MNCs were used without stimulation.
82 Cells were washed once with PBS and then surface-stained for CD9.

83 Surface-stained cells were washed once with PBS and fixed by 2% paraformaldehyde (Aldrich)/PBS at
84 37 °C for 10 min. Cells were permeabilized with 90% ice cold methanol in PBS/2% FBS/0.2% Tween-
85 20 for 30 min at 4 °C. Subsequent washing steps were performed with PBS/2% FBS/0.2% Tween-20.
86 Cells were washed twice and incubated with phospho-STAT5-APC or STAT5 and Streptavidin-PE/Cy7
87 (if a biotinylated surface antibody was used) antibodies on ice for one hour. Cells incubated with the
88 STAT5 antibody were washed twice and then incubated with IgG-APC (H+L) on ice for 20 min. Cells
89 were washed two times before analysis via flow cytometry.

90 *qPCR analyses*

91 RNA was isolated using the RNeasy MiniKit according to the manufacturer's instructions. RNA was
92 transcribed with the iSCRIPT cDNA synthesis kit. Quantitative real-time PCR was performed on a
93 CFX96 Real-Time System C1000Touch Thermal Cycler (Bio-Rad) with SsoAdvanced universal SYBR
94 GreenSupermix. Murine mRNA levels of *Socs2*, *Cish*, *Meg3*, *Ifitm1*, *Ifitm3*, *Stat1*, *Cd9*, *Rplp0* were
95 analysed. Target gene expression was normalized to expression of Ribosomal Protein Lateral Stalk
96 Subunit P0 (Rplp0).

97 *Cytoplasmic and nuclear fractionation*

98 1×10^7 SET2 or HEL cells were washed once with PBS OR 2×10^7 HPC^{LSK} cells stimulated with either
99 10 U/ml EPO, 100 ng/ml GM-CSF, 100 ng/ml IL-3 or 100 ng/ml TPO for 20 min at 37 °C or left
100 unstimulated. Cells were washed once with PBS OR 2×10^7 HPC^{LSK} cells retro-virally expressing FLT3-
101 ITD or BCR/ABL^{p210} and HPC-7 cells retro-virally expressing JAK2^{V617F} were washed once with PBS.
102 All steps were performed at 4 °C. Cells listed above were resuspended in Buffer A (10 mM HEPES pH
103 7.9, 10 mM KCl, 0.1 mM EDTA, 0.1 mM EGTA, 2 mM DTT, 0.4 mM Na-Vanadate, 25 mM Na-
104 Fluoride, 1 mM PMSF, 20 µg/ml Leupeptin and 20 U/ml Aprotinin) and incubated for 15 min on ice.
105 10% NP-40 was added, vortexed and cytoplasmic supernatant was collected after centrifugation at
106 13,000 g for 1 min. The pellet was washed 5 times with pre-cooled PBS and resuspended in Buffer B
107 (20 mM HEPES pH 7.9, 25% Glycerol, 400 mM NaCl, 1 mM EDTA, 1 mM EGTA, 2 mM DTT, 0.4
108 mM Na-Vanadate, 25 mM Na-Fluoride, 1 mM PMSF, 20 µg/ml Leupeptin and 20 U/ml Aprotinin) and
109 incubated for 1h at 4°C while shaking. Nuclear supernatant was collected after centrifugation at 13,000
110 g for 5 min.

111 *Immunoprecipitation*

112 Whole cell lysates were harvested as described⁵. 300µg protein lysates of HEL, K562, SET2 or 1mg
113 protein lysates of HPC^{LSK} cells were incubated at 4°C o/n while rotating with either STAT5A or
114 STAT5B antibody in radioimmunoprecipitation assay (RIPA) buffer. Next day, SureBeadsTM Protein
115 Magnetic Beads were added and incubated for 2h at 4°C while rotating. Beads were washed three times
116 with pre-cooled RIPA buffer and then eluted with 4x Laemmli buffer for 5min at 95°C. Eluates were
117 loaded for immunoblot analyses.

118 *Immunoblotting*

119 Proteins were separated on an 8% SDS polyacrylamide gel and transferred to nitrocellulose membranes.
120 The following antibodies were used for immunoblotting: STAT5A, STAT5B, STAT5A/B, pSTAT5
121 (Y694/699). α -TUBULIN or RCC1 served as loading control. Anti-mouse and anti-rabbit HRP
122 conjugated secondary antibodies were used. Chemiluminescent visualisation was performed with a
123 ChemiDoc™ Touch Imaging System after incubation of the membranes with Clarity Western ECL
124 reagent.

125 *Chromatin Immunoprecipitation (ChIP) - qPCR*

126 2.5×10^7 HPC^{LSK} cells were either stimulated with 100 ng/ml TPO or left unstimulated for 30min. Cells
127 were washed once with PBS and crosslinked with 2 mM DSG in PBS for 30 min at RT, washed twice
128 and incubated with 1% Formaldehyde in PBS for 10 min at RT. Cell lysis and sonication was performed
129 as described in⁶. Sheared chromatin was incubated with 5 μ g anti-STAT5B or anti-IgG (as control)
130 antibodies overnight at 4 °C and processed as described in⁶. Selected pulled down genomic regions were
131 quantified by quantitative real-time PCR performed on a CFX96 Real-Time System C1000Touch
132 Thermal Cycler with SsoAdvanced universal SYBR GreenSupermix. The following genomic regions
133 were analysed: *Cd9 Prom*, *Cd9 neg1*, *Cd9 neg2*, *Cish bdg*, *Cish neg*, *Bcl2-l1 bdg* and *Bcl2-l1-neg*.

134 *Immunohistochemistry (IHC)*

135 Cytospins of 5×10^4 HPC^{LSK} wt cells (unstimulated or stimulated for 20min with TPO) were fixed for 5
136 min in ice-cold Methanol and air-dried. Retrieval step of slides was performed in 0.01 M citric acid (pH
137 6.95) in a water bath at 95 °C for 10 min. Slides were washed three times with PBS and then
138 permeabilized with 0.1% TritonX-100 in PBS for 10 min. Slides were washed two times and blocked
139 with 10% goat serum for 30 min. STAT5A (for IHC, 1:500) or STAT5B (1:100) antibody was incubated
140 in PBS containing 2% goat serum at 4 °C o/n. Slides were washed two times and incubated with
141 biotinylated secondary antibody (from VECTASTAIN® Elite® ABC HRP Kit) in PBST containing
142 2% goat serum for 30 min at RT. Slides were washed two times with PBST and then incubated with
143 ABC solution (VECTASTAIN® Elite® ABC HRP Kit) for 45 min at RT. Slides were washed two times
144 and counter-stained with Hemalaun for 90 s. After wash step with tap water slides were mounted with
145 Aquatex. Pictures were taken with an OLYMPUS IX71 inverted microscope using the CellSens
146 Dimension software with an OLYMPUS DP72 camera. For nuclear STAT5A/B staining intensity
147 quantification, high-power field sections (x200 objective) were obtained for each sample and analysed
148 with HistoQuest (TissueGnostics GmbH) quantification software as described⁷.

149 *in vitro experiments*

150 *Analyses of CD9 levels*

151 1.5×10^6 HPC^{LSK} cells were treated with 100 ng/ml TPO in culture conditions for 30 min, 2 h, 24 h or
152 left unstimulated. Cells were washed once with PBS and mRNA levels were analysed by qPCR (see
153 above) or 3×10^6 wt, *Stat5a*^{-/-} or *Stat5b*^{-/-} BM cells were stimulated with 100 ng/ml TPO in IMDM, 5%
154 FBS, 15 mM monothioglycerol (MTG), 2 mM L-Glutamine and cultured for up to 96 h. TPO was added
155 every 24 h. Cells were analysed for CD9 levels on LSK cells via flow cytometry every 24 h or HPC^{LSK}

156 cells retro-virally expressing FLT3-ITD or BCR/ABL^{p210} and HPC-7 cells expressing FLT3-ITD or
157 JAK2^{V617F} were analysed for CD9 levels via flow cytometry.

158 *Single HSC-derived culture*

159 FACS-sorted single HSC/MPP1 (LSK, CD150⁺, CD48⁻) cells obtained from wt, *Stat5a*^{-/-} and *Stat5b*^{-/-}
160 mice were cultured in IMDM, 5% FBS, 15 mM MTG, 2 mM L-Glutamine, 2% SCF and 25 ng/ml TPO.
161 After 10 days, single cell-derived clones were analysed via flow cytometry for clonal outgrowth,
162 numbers of LSK and total cells.

163 *LSK-derived culture*

164 1x10⁴ LSK cells obtained from wt, *Stat5a*^{-/-} or *Stat5b*^{-/-} mice were FACS-sorted and cultured in IMDM,
165 5% FBS, 15 mM MTG, 2 mM L-Glutamine, 2% SCF and 25 ng/ml TPO. Cells were analysed via flow
166 cytometry for total cell numbers after 4, 7, 10 and 15 days.

167 *Stat5a/b over-expression in LSK culture*

168 5x10³ LSK cells obtained from wt mice were FACS-sorted and infected with a pMSCV-IRES-GFP-
169 based construct encoding *Stat5a* or *Stat5b* as described⁸. Infections with the empty vector (eV) served
170 as control. Infections were performed in IMDM, 5% FBS, 15 mM MTG, 2 mM L-Glutamine, 2% SCF,
171 25 ng/ml TPO, 10 ng/ml IL-3 and 10 ng/ml IL-6. Upon two days of infection, medium was exchanged
172 to IMDM, 5% FBS, 15 mM MTG, 2 mM L-Glutamine, 2% SCF and 25 ng/ml TPO. Cells were analysed
173 via flow cytometry for GFP expression and total cell numbers after 5, 7, 10, 15, 20, 25 and 29 days and
174 for LSK markers after 28 days.

175 *LSK Re-plating*

176 1x10³ FACS-sorted LSK cells obtained from wt, *Stat5a*^{-/-} or *Stat5b*^{-/-} mice were cultured in IMDM, 5%
177 FBS, 15 mM MTG, 2 mM L-Glutamine, 2% SCF and 25 ng/ml TPO. After 2 days all cells were
178 harvested and seeded in methylcellulose (MethoCult 03231) supplemented with 10 ng/ml IL3, 10 ng/ml
179 IL6, 5 U/ml EPO (3 U/ml), 0.5% SCF, 200 µg/ml transferrin and 10 µg/ml Insulin. Colonies were
180 counted after 8 days, liquefied with PBS and analysed via flow cytometry for total cell numbers. 3x10⁴
181 cells were seeded again in methylcellulose (MethoCult 03231) supplemented with cytokines as
182 described above. Colonies were counted after 8 days.

183 *HPC^{LSK} Re-plating – over-expressing eV, STAT5B, STAT5B^{N642H}*

184 1.25x10³ HPC^{LSK} cells retro-virally expressing STAT5B, STAT5B^{N642H} or empty vector (eV, as control)
185 were harvested and seeded in methylcellulose (MethoCult 03231) supplemented with 0.3% SCF.
186 Colonies were counted after 10 days, liquefied with PBS and analysed via flow cytometry for total cell
187 numbers. This procedure was repeated for up to 3 serial platings.

188 **CD9 blocking experiments**

189 *Colony formation assays (murine)*

190 5x10⁵ wt or JAK2^{V617F}, vav-Cre BM cells were treated with 5 µg/ml aCD9 or IgG antibodies and seeded
191 in methylcellulose (MethoCult, 03231) supplemented with 20 ng/ml IL-3, 20 ng/ml IL-6, 5 U/ml EPO

192 (3 U/ml), 0.5% SCF, 200 µg/ml transferrin and 10 µg/ml insulin. Colonies were counted after 12 days,
193 liquefied with PBS and analysed via flow cytometry for total and LSK cell numbers and for levels of c-
194 kit and CD11b.

195 *Liquid culture (murine)*

196 2.5×10^5 wt or JAK2^{V617F}, vav-Cre BM cells were treated with 2 µg/ml aCD9 or IgG antibodies and
197 cultured in IMDM with 5% FBS, 15 mM MTG, 2 mM L-Glutamine for 2 days. Cells were analysed for
198 Annexin-V levels, total and LSK cell numbers.

199 *Liquid culture - aCD9: KMC8 vs. MZ3 (murine)*

200 3×10^6 JAK2^{V617F}, vav-Cre BM cells were treated with either 5 µg/ml aCD9 (KMC8), aCD9 (MZ3) or
201 IgG antibodies and cultured in IMDM, 5% FBS, 15 mM MTG, 2 mM L-Glutamine, 2% SCF, 25 ng/ml
202 TPO, 10 ng/ml IL-3 and 10 ng/ml IL-6 for 4 days. Cells were analysed by flow cytometry for Annexin-
203 V and CD9 levels, as well as for total and LSK cell numbers.

204 *Liquid culture - aCD9 vs. AC-4-130*

205 3×10^6 JAK2^{V617F}, vav-Cre BM cells were treated with either 5 µg/ml aCD9 or IgG antibodies or with 5
206 µM AC4-130⁹ or respective amount of DMSO and cultured in IMDM, 5% FBS, 15 mM MTG, 2 mM
207 L-Glutamine, 2% SCF, 25 ng/ml TPO, 10 ng/ml IL-3 and 10 ng/ml IL-6 for 4 days. Cells were analysed
208 by flow cytometry for Annexin-V, c-kit, and CD9 levels, as well as for total and LSK cell numbers.

209 *Intracellular staining – aCD9 affects pYSTAT5 levels*

210 3×10^6 JAK2^{V617F}, vav-Cre BM cells were treated with either 5 µg/ml aCD9 or IgG antibodies and
211 cultured in IMDM, 5% FBS, 15 mM MTG, 2 mM L-Glutamine. After 1 h treatment, cells were
212 stimulated with 100ng/ml TPO, 100 ng/ml GM-CSF, 10 U/ml EPO or 100 ng/ml IL-3 for 15min. Cells
213 were washed once in PBS and surface-stained for CD150⁺CD48⁻LSK cells following intracellular
214 staining for pYSTAT5.

215 **CD9 blocking experiments – patient samples**

216 *Liquid culture*

217 5×10^5 AML^{FLT3-ITD⁺}, CML^{BCR/ABL1⁺} or MPN^{JAK2V617F} patient-derived BM MNC (listed in Supplementary
218 **Table S2**) were treated with 2 µg/ml aCD9 or IgG antibodies and cultured in IMDM with 5% FBS, 15
219 mM MTG, 2 mM L-Glutamine for 2 days. AML^{FLT3-ITD⁺} and CML^{BCR/ABL1⁺} were maintained without
220 cytokines, while MPN^{JAK2V617F} BM MNCs were maintained with 100 ng/ml hSCF, 10 ng/ml hIL-3, 25
221 ng/ml hTPO, 5 U/ml EPO. After 2 days cells were analysed for CD45⁺ and CD34⁺CD38⁻ cell numbers,
222 Annexin-V, CD11b and CD34 levels.

223 *Serial plating*

224 6×10^4 MPN^{JAK2V617F⁺} BM cells were treated with 10 µg/ml aCD9 or IgG antibodies and seeded in
225 methylcellulose (MethoCult 04431). Colonies were counted after 14 days, liquefied with PBS and
226 analysed via flow cytometry for total and CD34⁺CD38⁻ cell numbers. 3×10^4 cells were again treated
227 with 10 µg/ml aCD9 or IgG antibodies, and seeded in methylcellulose and as described above. Colonies

228 were counted after 20 days. 6×10^4 CML^{BCR/ABL1+} BM cells were treated with 5 μ g/ml aCD9 or IgG
229 antibodies and seeded in methylcellulose (MethoCult 04435). Colonies were counted after 11 days.
230 3×10^4 cells were again treated with 5 μ g/ml aCD9 or IgG antibodies, and seeded in methylcellulose as
231 described above. Colonies were counted after 23 days. Colonies were always liquefied with PBS and
232 analysed via flow cytometry for total and CD34⁺CD38⁻ cell numbers.

233 *Liquid culture - non-toxicity test*

234 5×10^5 control human patient BM MNC (listed in Supplementary **Table S2**) were treated with either 2
235 μ g/ml, 5 μ g/ml or 10 μ g/ml aCD9 or IgG antibodies and cultured in IMDM with 5% FBS, 15 mM MTG,
236 2 mM L-Glutamine for 2 days. Cells were analysed for CD45⁺ and CD34⁺CD38⁻ cell numbers.

237 *Serial plating – non-toxicity test*

238 6×10^4 control human patient BM MNC (listed in Supplementary **Table S2**) were treated with either 2
239 μ g/ml, 5 μ g/ml or 10 μ g/ml aCD9 or IgG antibodies and seeded in methylcellulose (MethoCult 04431).
240 After 14 days, colonies were liquefied with PBS and analysed via flow cytometry for CD45⁺ and
241 CD34⁺CD38⁻ cell numbers.

242 ***in vivo* experiments**

243 *5-FU injection*

244 wt, *Stat5a*^{-/-} and *Stat5b*^{-/-} mice (6-10 weeks of age) were injected i.p. with 150 mg/kg 5-FU (resolved in
245 200 μ l physiological sodium chloride solution). BM cells were analysed for total cell numbers, the
246 presence of individual LSK populations, cell cycle distribution and apoptosis 8 days post treatment.

247 *Serial transplantation assays*

248 5×10^6 BM cells derived from wt (*Ly5.2*⁺), *Stat5a*^{-/-} (*Ly5.2*⁺) and *Stat5b*^{-/-} (*Ly5.2*⁺) mice were injected
249 intravenously (i.v.) into lethally irradiated (9 Gy) C57Bl/6J (*Ly5.1*⁺) recipient mice. The irradiated
250 control mice had to be sacrificed after 9 days. For the assessment of long-term repopulation capacities
251 of transplanted HSCs, mice were euthanized 16 weeks post-transplantation. BM was analysed by flow
252 cytometry for the contribution of *Ly5.1*⁺ and *Ly5.2*⁺ cells to individual HSC populations and total cell
253 numbers. 5×10^6 of collected BM cells were re-injected in lethally irradiated (9 Gy) C57Bl/6J (*Ly5.1*⁺)
254 mice This procedure was repeated up to four rounds of transplantation.

255 *Serial transplantation of BCR/ABL^{p210+} LSK cells*

256 FACS-sorted LSK cells from wt, *Stat5a*^{-/-} and *Stat5b*^{-/-} BM were infected with BCR/ABL^{p210-GFP} virus-
257 containing supernatant as previously described¹⁰. Two days post infection, 2×10^4 GFP⁺ LSK cells were
258 injected i.v. in NOG mice. When the first recipient showed signs of disease, four mice per genotype
259 were euthanized, analysed by flow cytometry for total cell numbers, LSK and lineage populations and
260 2.5×10^4 GFP⁺ cells were re-injected i.v. in NSG mice. In both rounds of transplantation, recipients were
261 sacrificed upon first signs of disease (paralysis of hind legs) and analysed for total GFP⁺ and GFP⁺ LSK
262 cell numbers.

263 *JAK2^{V617F} BM Transplantation – aCD9 pre-treatment*

264 5×10^6 BM cells derived from $JAK2^{V617F}$ ($Ly5.2^+$) mice were treated *in vitro* with 5 μ g/ml aCD9 or IgG
265 in IMDM supplemented with in IMDM, 5% FBS, 15 mM MTG, 2 mM L-Glutamine, 2% SCF, 25 ng/ml
266 TPO, 10 ng/ml IL-3 and 10 ng/ml IL-6 for 24 h. After a viability check using a live/dead dye
267 (SytoxBlue), cells were injected i.v. in NSG mice ($Ly5.1^+$, 4 mice per condition) Three weeks after
268 transplantation, spleen size and $Ly5.2^+$ HSC and total cell numbers (flow cytometry) were analysed.

269 $JAK2^{V617F}$ BM Transplantation – *in vivo* aCD9 treatment

270 5×10^6 BM cells from $JAK2^{V617F}$ ($Ly5.2^+$) mice were injected i.v. in NSG mice ($Ly5.1^+$, n=8). One week
271 thereafter, the recipients ($Ly5.1^+$) were treated 4 times (4-day-interval) with aCD9 or IgG i.v. (1.25
272 mg/kg, 4 mice per condition). Four weeks after the treatment, the recipient mice were analysed for spleen
273 size and by flow cytometry for $Ly5.1^+$ and $Ly5.2^+$ HSC and total cell numbers.

274 **Single cell RNA-Seq (10x genomics)**

275 LSK cells were sorted from tibiae and femora of wt, $Stat5a^{-/-}$ or $Stat5b^{-/-}$ mice were subjected to single
276 cell RNA-seq profiling using the 10X Genomics Chromium Single Cell Controller and sequenced on an
277 Illumina Hi-Seq3000/4000 system. Further details are listed in the supplementary information. These
278 data can be accessed in the GEO database, accession number GSE178648.

279 Mouse BM cells of wt, $Stat5a^{-/-}$ or $Stat5b^{-/-}$ mice were recovered from femora and tibiae in PBS. The cell
280 suspension was filtered through a 70 μ m cell strainer, washed once in PBS and frozen at -150 $^{\circ}$ C,
281 according to “10x Genomics Sample Preparation Demonstrated Protocol” (CG00039). Three samples
282 of wt, $Stat5a^{-/-}$ or $Stat5b^{-/-}$ BM were thawed and 3×10^4 LSK cells per genotype were FACS sorted
283 individually at the core facility flow cytometry of the Medical University of Vienna using the lineage
284 cocktail of antibodies including (anti-mouse CD3; anti-mouse Ly-6G/Ly-6C; anti-mouse CD11b; anti-
285 mouse CD45R/B220; anti-mouse TER-119), anti-mouse Ly6A/E (Sca-1) and anti-mouse CD117 (c-kit).
286 FACS-purified cells were harvested in PBS with 0.04% BSA and subjected to single cell RNA-seq
287 profiling using the 10X Genomics Chromium Single Cell Controller with the Chromium Single cell 3’
288 Kit v1 following the manufacturers’ instructions. Successful libraries were quality controlled using the
289 QBit system for quantification and the Agilent Bioanalyzer for fragment length verification and
290 sequenced on an Illumina Hi-Seq3000/4000 system with the 75bp paired end setting.

291 *Single cell RNA-Seq: Sample demultiplexing, barcode processing and UMI counting*

292 The 10x Genomics Cell Ranger pipeline 3.0.2 was used for sample demultiplexing, barcode processing
293 and UMI counting. Reads were aligned to the mouse reference genome (version refdata-cellranger-
294 mm10-3.0.0). Each library was processed separately using the CellRanger count tool to generate gene x
295 barcode matrices.

296 *Single cell RNA-Seq: Data cleaning and normalization*

297 The R package Seurat v3^{11,12} was used to analyze the data. Gene-barcode matrices were imported into
298 Seurat and normalized and scaled with default settings. To remove cells with low sequencing quality,
299 cutoffs for a minimal number of detected genes and UMI per cell were defined based on visualizations

300 of the distributions of the number of detected genes and UMI per cell for each sample. Potential doublets
301 were identified using the following approach: normalized and scaled expression values of detected genes
302 on sex chromosomes were used for dimension reduction by Uniform Manifold Approximation and
303 Projection (UMAP). The first two UMAP dimensions were then used to find k nearest neighbors and
304 construct a Shared Nearest Neighbor (SNN) graph which was then used for clustering. For that purpose
305 the FindNeighbors (default settings) and FindClusters (resolution = 0.01) functions implemented in
306 Seurat were used. In each sample, a cluster with a higher mean number of detected genes per cell as well
307 as a higher median UMI per cell than the other clusters was identified. These clusters contain potential
308 doublets and were removed. After filtering, 8036 *Stat5a*^{-/-}, 8347 *Stat5b*^{-/-}, and 6564 wt cells were
309 preserved. Raw counts of kept cells were again normalized using the NormalizeData function of Seurat
310 with default settings, and the top 2000 most variable genes were determined using Seurat's
311 FindVariableFeatures function (default settings).

312 *Data integration and removing of contaminating cell clusters*

313 Filtered and normalized samples were integrated using Seurat's "FindIntegrationAnchors"- and
314 "IntegrateData"-functions (both with standard parameters). First, we checked for potential
315 contaminating cell populations. For that purpose data was scaled (Seurat's "ScaleData"-function; all
316 genes were used for scaling), dimensions reduced (Seurat's "RunPCA"; default settings), KNN
317 calculated and used for SNN graph construction (Seurat's "FindNeighbors"; dims = 1:20), and clusters
318 defined (Seurat's "FindClusters"; resolution = 0.5). Visualization of these clusters on the first two
319 dimensions from UMAP (Seurat's "RunUMAP" on first 20 principal components) identified small
320 clusters localized far away from the bulk of cells representing potential contaminations. Removing of
321 these contaminating clusters (by visual inspection of clusters in the UMAP and filtering accordingly)
322 resulted in 6726 *Stat5a*^{-/-}, 7350 *Stat5b*^{-/-}, and 4904 wt cells.

323 *Removing cell cycle genes from integration analysis*

324 In addition to contaminating clusters, the UMAP plot showed a distinct group of cells, composed of two
325 clusters, which mapped away from the rest of the cells. Marker gene identification revealed that these
326 cells showed high expression of a G2-M cell cycle signature (data not shown).

327 In an attempt to identify clusters based on genes related to cell type rather than cell cycle state, cell
328 cycle-related genes were removed from the clustering analysis. Inspired by a similar analysis¹³, we
329 categorised genes as cell-cycle related if they were part of the Gene Ontology (GO) set "mitotic cell
330 cycle process" (GO:1903047). First, any gene from the 2500 anchor features that was found in the GO
331 set, was removed from the anchor features list. Second, all genes from the remaining anchor features
332 that were highly correlated with at least one of the cell cycle genes in the GO set were removed, too. To
333 do the latter, Pearson correlation coefficients were calculated between any remaining anchor feature and
334 the genes that were part of the GO set. Features that had a maximum Pearson correlation coefficient of
335 greater than or equal to 0.15 between themselves and any gene of the GO set, were excluded from the

336 anchor features, too. After this procedure 1963 genes remained in the integration anchors list and were
337 used for re-integration of the data.

338 *Re-integration of datasets, cluster identification and force directed graph representation*

339 The three data sets were re-integrated using the 1963 remaining anchor features and the wildtype sample
340 as a reference. The newly integrated data were again scaled and PCA (default parameters) and UMAP
341 (with dims = 1:30) dimensionality reductions were performed. A separation of subgroups of cells as
342 observed before was not apparent in this analysis. We next calculated the k=7 nearest neighbours (KNN)
343 and from that shared nearest neighbours (SNN) as implemented in the FindNeighbors function in Seurat.
344 The SNN were used to identify clusters (FindClusters function with a resolution parameter of 0.9).
345 For visualization, the KNN graph was exported and the data were used to generate a force directed graph
346 (using Gephi 0.9.2 with the Force Atlas 2 layout). The force directed graph was imported into R and
347 added to the Seurat analysis object as a dimensional reduction object and used for visualization of the
348 data.

349 For visual comparison of force directed graphs from the three samples the cell numbers were adjusted
350 such that each plot showed 4904 cells (all cells for the wild-type sample, random samples for the other
351 two). Force directed graphs were also used to visually inspect the expression of cluster marker genes
352 (FeaturePlot function with min.cutoff = "q20", max.cutoff = "q95").

353 *Cluster marker genes, cluster annotation, cluster heatmap*

354 Cluster-specific maker genes (Supplementary **Table S3**) were identified using Seurat's
355 FindConservedMarker function. These marker genes allowed for the manual annotation of clusters as
356 being enriched for individual hematopoietic progenitor cell types. A random sample of 2000 cells was
357 drawn in order to generate a heatmap demonstrating marker gene expression. Genes to be plotted were
358 chosen as follows: The marker gene lists for each cluster were sorted by maximum p-value (low to high)
359 and possible ties were sorted by fold change of the wt sample (high to low). The top ranking genes with
360 a maximum p-value of $< 1e-10$ were plotted for each cluster, up to a total of 20 genes per cluster.

361 *Single cell RNA-Seq: Comparison of cluster sizes*

362 Relative cluster sizes were calculated for each sample separately as the percentage of the cells within a
363 cluster. Differences between samples were calculated as log₂ fold change between *Stat5a*^{-/-} and wt as
364 well as *Stat5b*^{-/-} and wt.

365 *Label-Transfer*

366 We downloaded the data from Gene Expression Omnibus (GEO accession: GSE107727) and processed
367 six samples (the three LSK and the three LK samples) following the methods described in Dahlin *et al.*
368 2018¹³. We reproduced their analysis and then performed Louvain clustering to identify 16 clusters and
369 annotated them for hematopoietic stem and progenitor cell types following Dahlin *et al.* where possible.
370 Clusters that did not receive a label in the original publication were not labelled by us either - except for
371 one cluster adjacent to the HSC cluster, which we labelled "adjacent_HSC" (**Figure S11**). We performed
372 the label-transfer onto our dataset, following the standard label-transfer workflow

373 (<https://satijalab.org/seurat/archive/v3.0/integration.html>, “Standard Workflow”, 09.07.2021) using
374 default parameters.

375 *Single cell RNA-Seq: Cell cycle score*

376 Cell cycle phases were assigned to cells using the cyclone function¹⁴ from the package scran with default
377 parameters. The provided pre-trained classifier for mouse was used.

378 *Single cell RNA-Seq: Identification of a Stat5b specific stem cell signature*

379 Markers for HSCs were downloaded from CellMarker database
380 (<http://biocc.hrbmu.edu.cn/CellMarker/download.jsp>). Genes from studies PMIDs 27580035,
381 28479188, 27225119 and 29915358 detected in any cell of our scRNA-seq were included (577 unique
382 genes).

383 The mean expression of the HSC marker genes scaled within cells of one genotype was calculated for
384 each cell and used to classify cells into HSC signature high (top10% = “HSC-high”) and low (“HSC-
385 low”) cells. Differential expression analysis between HSC-high and HSC-low cells was performed for
386 each genotype using the FindMarker function (logfc.threshold = 0, min.pct = 0). Only genes detected in
387 at least 10% in any of the analyzed groups and significantly higher expressed in HSC-high cells in all
388 genotypes (adjusted p value < 0.05) were included for further analysis. In order to discriminate between
389 Stat5b and Stat5a effects, we looked for genes with opposing effects in both genotypes. 35 genes were
390 downregulated in *Stat5b*^{-/-} and up-regulated in *Stat5a*^{-/-} compared to wt, and 2 genes were up-regulated
391 in *Stat5b*^{-/-} and down-regulated in *Stat5a*^{-/-}.

392 *Gene Set Enrichment Analysis (GSEA)*

393 FindMarkers function from Seurat (logfc.threshold = 0, min.pct = 0, min.cells.feature = 1,
394 min.cells.group = 1) was used to perform differential gene expression analysis (DEA) of clusters HSC_1
395 and HSC_2 between wt, *Stat5a*^{-/-} and *Stat5b*^{-/-} cells. GSEA was performed using fGSEA version 1.14.0
396 with ranked gene lists (sign of fold change * -log₁₀(p-value)) of different DEAs (*Stat5a*^{-/-} vs. wt; *Stat5b*^{-/-}
397 vs. WT; *Stat5b*^{-/-} vs. *Stat5a*^{-/-}) and gene sets from CellMarker-database (obtained from Clustermole
398 version 1.0.1).

399 **Publicly available gene expression data sets**

400 For survival analysis of STAT5B-specific HSC genes, the gene expression data sets GSE6891,
401 GSE37642, GSE13159, GSE76008 and GSE63270 were obtained from GEO database and data set
402 OHSU was obtained by cBioPortal for Cancer Genomics¹⁵. Raw Affymetrix gene expression data were
403 processed, normalised and log₂ transformed using the frozen robust multiarray (fRMA) algorithm and
404 R 3.4.2 software¹⁶. Pre-processed Illumina BeadArray data (GSE76008) and RNA-seq data (OHSU)
405 were used as provided by the databases. Differential expression was calculated using the lmFit function
406 of the R package limma and an FDR<0.05 was considered statistically significant. Optimal cut points to
407 stratify samples into CD9-high and CD9-low for survival analyses were calculated using maximally
408 selected rank statistics (R package maxstat) as previously described¹⁷. Statistical significance between

409 these groups was assessed through the log-rank test. Survival analyses and visualization were performed
 410 using the R packages survival and survminer.

411 *Processing of published RNA-seq data*

412 For expression visualization of genes of interest we analysed a published RNA-seq dataset of FACS
 413 sorted HSC subpopulations (E-MTAB-2262)¹⁸. Briefly, raw FASTQ files were trimmed with
 414 Trimmomatic (version 0.36) and quality checked before and after trimming using FastQC. Next reads
 415 were mapped to the GENECODE M13 genome using STAR (version 2.5.2b) with default parameters.
 416 Counts for union gene models were obtained using featureCounts from the Subread package (version
 417 1.5.1). Regularized, log-transformed counts (DESeq2 (version 1.28.1)) were used for plotting.

418 **Supplementary Table S1: Resource Table**

REAGENT or RESOURCE	SOURCE	IDENTIFIER
<i>Antibodies</i>		
<i>Antibodies used for Immunoblotting, IP, ChIP, IHC or blocking experiments</i>		
STAT5A	R&D	MAB2174
STAT5A (for IHC)	Abcam	Ab32043
STAT5B	Abcam	Ab178941
Rabbit IgG	Abcam	Ab17273
pSTAT5 (Y694/699)	BD	611965
STAT5A/B	R&D	AF2168
A-TUBULIN	CST	21255
RCC1	Santa Cruz	Sc-55559
Anti-human CD9 Monoclonal Antibody	eBioscience	SN4 C3-3A2
CD9 Rat anti-Mouse	eBioscience	eBioKMC8
Purified anti-mouse CD9 Antibody	Biozym	(DRAP-27, MRP-1, p-24), clone: MZ3
Rat IgG2a kappa Isotype Control	eBioscience	eBR2a
Mouse IgG1 kappa Isotype Control	eBioscience	P3.6.2.8.1
<i>Murine antibodies for flow cytometry</i>		
TER119-APC/Cy7	Invitrogen	TER-119
Gr1-APC	Biozym	RB6-8C5
CD19-APC/Cy7	eBioscience	eBio1D3
CD3-APC/Cy7	Biozym	17A2
CD11b-APC/Cy7	Invitrogen	M1/70
Sca1-PE/Cy7	eBioscience	D7
c-kit-PE/Cy5	Invitrogen	2B8
CD150-APC	Biozym	TC15-12F12.2
CD48-PE	Biozym	HM48-1

CD135-Biotin	eBioscience	A2F10
CD34-FITC	eBioscience	RAM34
CD9-PB	Invitrogen	KMC8
CD19-PB	eBioscience	eBIO1D3
Gr1-PB	Invitrogen	RB6-8C5
CD11b-PB	eBioscience	M1/70
TER-119	eBioscience	TER-119
CD3-PB	Biozym	17A3
c-kit-FITC	Biozym	2B8
CD150-BV521	Biozym	TC15-12F12.2
Sca1-Biotin.	Biozym	D7
Streptavidin-PE/Cy7	Biozym	Streptavidin
Streptavidin-PB	eBioscience	Streptavidin
CD45R-PE	BD	RA3-6B2
CD3-FITC	BD	17A2
Gr1-FITC	BD	RB6-8C5
CD11b-PE/Cy7	eBioscience	M1/70
CD71-FITC	Invitrogen	R17217
CD41-Biotin.	eBioscience	eBioMWRReg30
CD41-PB	Biozym	MWRReg30
Ly5.1-PE	Biozym	A20
Ly5.1-FITC	Biozym	A20
Ly5.2-FITC	eBioscience	104
Ly5.2-PB	eBioscience	104
CD93-APC	Invitrogen	AA4.1
CD43-Biotin	BD	S7
Streptavidin BV650	Biozym	Streptavidin
CD19-BV605	Biozym	6D5
CD127-PB	eBioscience	A7R34
Phospho-STAT5-APC	BD	47/Stat5(pY694)
IgG-APC (H+L)	Invitrogen	Polyclonal
STAT5	CST	D2O6Y
AnnexinV-FITC	BD	556420
FITC Mouse Anti-KI67 Set	BD	556026
<i>Human Antibodies for flow cytometry</i>		

CD34-PE	Biozym	581
CD38-PE/Cy7	Biozym	Kappa HB-7
CD11b-APC/Cy7	Biozym	ICRF44
CD45-PB	eBioscience	HI30
CD9-FITC	Invitrogen	eBioSN4
Cytokines		
<i>Murine Cytokines</i>		
IL-2	PeproTech	212-12
IL-3	R&D	403-ML
IL-6	R&D	406-ML
IL-7	R&D	407-ML
GM-CSF	R&D	415-ML
TPO	PeproTech	315-14-100UG
EPO	Janssen	ERYPO® FS
SCF	VetMed	
<i>Human Cytokines</i>		
hIL-3	PeproTech	AF-200-03-100UG
hSCF	PeproTech	AF-300-07-100UG
hTPO	PeproTech	300-18
EPO	Janssen	ERYPO® FS
Chemicals, Peptides, and Recombinant Proteins		
Disuccinimidyl Glutarate	Thermo Scientific	20593
16% Formaldehyde solution (w/v), Methanol-free	Thermo Scientific	28906
DNase type I	SIGMA	DN25-1G
TurboFect Transfection Reagent	Thermo Scientific	R0532
PenStrep	SIGMA	P4333-100ML
2-Mercaptoethanol	SIGMA	M3148-250ML
RPMI Medium	SIGMA	R8758-500ML
Fetal Bovine Serum (FBS)	Capricorn Scientific	FBS-12A
IMDM Medium	SIGMA	I3390-500ML
DMEM Medium	SIGMA	D6429-500ML
HEPES	SIGMA-ALDRICH	H0887-100ml
Aquatex Aqueous mounting medium	SIGMA-ALDRICH	1085620050
Mayer's hemalum solution	SIGMA-ALDRICH	1092491000
L-Glutamine	SIGMA-ALDRICH	G7513-100ML

Trypsin-EDTA Solution 1x	SIGMA	59417c
DAPI	SIGMA-ALDRICH	D9542
SytoxBBlue	Fisher Scientific	S34857
5-Fluorouracil (5-FU)	SANDOZ	L01BC02
Clarity Western ECL Substrate	BIO-RAD	1705061
Tween20	ROTH	9127.2
(Polybrene) Hexadimethrine Bromide	SIGMA	H9268-5g
SsoAdvanced universal SYBR GreenSupermix	BIO-RAD	1725275
AnnexinV Binding Buffer (10x)	Invitrogen	00-0055-56
Critical Commercial Assays		
MethoCult H4435 Enriched	StemCell Technologies	04435
MethoCult H4431 Enriched	StemCell Technologies	04431
MethoCult M3231	StemCell Technologies	03231
VECTASTAIN® Elite® ABC HRP Kit	Szabo Scandic	PK-6101
RNeasy MiniKit	Qiagen	74106
Qiagen MinElute PCR Purification Kit	Qiagen	28006
iSCRIPT cDNA synthesis kit	BIO-RAD	1708891BUN
Cytofix/Cytoperm Plus	BD	555028
Deposited Data		
GEO Single cell RNA-Seq in progress	hscs	
Experimental Models: Cell Lines		
gPp210 BCR/ABL ^{p210} retroviral producer cell line	VetMed	
K562	Kindly provided by Giulio Superti-Furga	
HEL	Kindly provided by Peter Valent	
SET2	Kindly provided by Peter Valent	
HPC-7	Kindly provided by Anthony Green	
HPC ^{LSK}	Generated in house	
Experimental Models: Organisms/Strains		
<i>Stat5a</i> ^{-/-}	VetMed	C57BL/6
<i>Stat5b</i> ^{-/-}	VetMed	C57BL/6
cS5A ^{hi}	VetMed	C57BL/6
STAT5B ^{N642H}	VetMed	C57BL/6
JAK2 ^{V617F}	VetMed	C57BL/6
Vav1-Cre	VetMed	C57BL/6
C57BL/6N	VetMed	C57BL/6

NOG-F		Taconic Biosciences	NOD.Cg-Prkdc ^{scid} Il2rgtm1Sug/JicTac
NSG		Charles River	NOD.Cg-Prkdc ^{scid} Il2rgtm ^{1Wj/SzJ}
Ly5.1 ⁺		Charles River	B6.SJL-Ptprca
Oligonucleotides			
<i>Murine Primer (qPCR)</i>	<i>forward (5'>3')</i>	<i>reverse (5'>3')</i>	<i>Origin</i>
<i>Socs2</i>	CAGTCAAACAGATGGTACTG	GGTAGTCTGAATGCGAACT ATCTC	Microsynth
<i>Cish</i>	CCTTCGGGAATCTGGGTGG	GACTGACAGTGTGAACAGG TAGC	Microsynth
<i>Meg3</i>	ACTCTTGCCACATTAGCCC	CACAGGAAGACGCGACAG	Microsynth
<i>Ifitm1</i>	GCCTATGCCTACTCCGTG	AGGATGGTGAAGAACAGGG A	Microsynth
<i>Ifitm3</i>	AGCCTATGCCTACTCCGTGA	GACCAAGGTGCTGATGTTC A	Microsynth
<i>Stat1</i>	CACATTCACATGGGTGGAAC	TCTGGTGCTTCCTTTGGTCT	Microsynth
<i>Cd9</i>	CTGGCATTGCAGTGCTTGCT A	AACCCGAAGAACAATCCCA GC	Microsynth
<i>Rplp0</i>	GCTTTCTGGAGGGTGTCC	GCTTCAGCTTTGGCAGGG	Microsynth
<i>Murine Primer (ChIP-qPCR)</i>	<i>forward (5'>3')</i>	<i>reverse (5'>3')</i>	<i>Origin</i>
<i>Cd9 Prom</i>	GTAGTCCCTAGAGCCTGCCT	TCCTGTGGCTTTGTGGTTGA	Microsynth
<i>Cd9 neg1</i>	GCTACTCCGCACCCTAACTC	GCCTTGCTCACTCACCTTCT C	Microsynth
<i>Cd9 neg2</i>	TCCTGGTGCAAACCTACCC	GACAGCAGTTGAGCAGACC TA	Microsynth
<i>Cish bdg</i>	CAACTCTAGGAGCTCCCGCC	AACACCTTTGACAGATTTCC AAGAAC	Microsynth
<i>Cish neg</i>	TACCCCTTCCAACCTCTGACTG AGC	TTCCCTCCAGGATGTGACT GTG	Microsynth
<i>Bcl2-11 bdg</i>	TGAGCTTCAGGGAATCTTTG GG	CCGCTTCCTGTTCTGAGAAA TG	Microsynth
<i>Bcl2-11 neg</i>	ACATACTGCCACTGAGTACCA C	TGAGAAGAGCCCAGCCTAA TTG	Microsynth
Recombinant DNA			
JAK2 ^{V617F} -GFP in pMSCV		Kindly provided by Richard Moriggl	
FLT3-ITD-GFP in pMSCV		Kindly provided by Richard Moriggl	
STAT5A-GFP in pMSCV		Kindly provided by Richard Moriggl	
STAT5B-GFP in pMSCV		Kindly provided by Richard Moriggl	
STAT5B-V5-GFP in pMSCV		Cloned in-house	
STAT5B ^{N642H} -V5-GFP in pMSCV		Cloned in-house	
Software and Algorithms			
GraphPad Prism (8.4.3.686)		GraphPad Software	
FlowJo (v10.6.1)		DeNovo Software	
Cytextpert (2.4.0.28)		Beckman Coulter	

FACSDiva	BD	
ImageJ	NIH	
ImageLab 5.2.1	BIO-RAD	
CellSens Dimension 1.5	OLYMPUS	
Adobe Photoshop CS5.1	Adobe	
Adobe Illustrator CS5.1	Adobe	
CFX Maestro 1.1 (4.1.2433.1219)	BIO-RAD	
CellRanger pipeline 3.0.2	10X Genomis	
R version 4.0.2		
Seurat version 3	Bioconductor	
scrn version 1.16.0	Bioconductor	
gephi 0.9.2	https://github.com/gephi/gephi	
Simpleaffy version 2.62.0	Bioconductor	
Frma version 1.38.0	Bioconductor	
Survival version 3.2-7	CRAN	
Survminer version 0.4.8	CRAN	
Ggpubr version 0.4.0	CRAN	
CellMarker database	http://biocc.hrbmu.edu.cn/CellMarker/download.jsp	
STAR version 2.5.2b	https://github.com/alexdobin/STAR	
FastQC	https://www.bioinformatics.babraham.ac.uk/projects/fastqc/	
Trimmomatic version 0.36	http://www.usadellab.org/cms/?page=trimmomatic	
Subread package version 1.5.1	http://subread.sourceforge.net/	
DESeq2 version 1.28.1	Bioconductor	
sva version 3.36.0	Bioconductor	
Histoquest 6.0.1.0127	TissueGnostics	
fgsea version 1.14.0	Bioconductor	
clustermole version 1.0.1	Bioconductor	
Other		
SureBeads™ Protein Magnetic Beads	BIO-RAD	161-4023

419

Supplementary Table S2: Information on primary patient samples

Nr	Sex	Date of Birth	Age	Diagnosis	FAB AML	% Blasts BM	Karyotype	Key Mutations / WHO
1	f	06.09.1940	79	CML CP	n.a.	1	46,XX,t(9;22)	BCR/ABL1: 35.1% IS
2	m	09.09.1992	27	CML CP	n.a.	0.5-1	n.a.	BCR/ABL1: 39.2% IS
3	f	01.11.1979	39	CML CP	n.a.	3	46,XX,t(9;22)	BCR/ABL1: 40.5% IS
4	f	29.10.1998	19	CML CP	n.a.	6	46,XX,t(9;22)	BCR/ABL1: 75.4% IS
5	m	22.09.1987	31	CML CP	n.a.	<2	46,XY,t(9;22)	BCR/ABL1: 27.9% IS
6	m	10.04.1948	70	CML CP	n.a.	2	46,XY,t(9;22)	BCR/ABL1: 68% IS
7	f	06.11.1965	53	MPN-PV	n.a.	<1	n.a.	JAK2 V617F+: 31.48%
8	f	29.07.1946	71	MPN/MDS	n.a.	2-3	46,XX, t(3;22)	JAK2 V617F+: 30.97%
9	f	04.04.1961	56	MPN-PV	n.a.	<1	46,XX	JAK2 V617F+: 16,32%
10	f	10.07.1976	42	MPN-ET	n.a.	<1	46,XX	JAK2 V617F+: 12.87%
11	f	19.04.1959	57	MPN-PV	n.a.	<1	46,XX	JAK2 V617F+: 53.56%
13	m	04.09.1962	53	AML (FLT3-ITD)	biphenotypic	90	46,XY	FLT3-ITD+
14	f	03.03.1965	51	AML (FLT3-ITD)	M1	95	46,XX	NPM1+, FLT3-ITD+
15	f	03.08.1972	44	AML (FLT3-ITD)	M1	80-85	46,XX	NPM1+, FLT3-ITD+
16	m	03.07.1967	50	AML (FLT3-ITD)	M4	67	46,XY,t(5;15)	NPM1+, FLT3-ITD+
18	m	10.02.1998	20	AML (FLT3-ITD)	M2/ AML with dysplasia	45	46,XY	NPM1+, FLT3-ITD+, KIT D816V, CEBPA
19	f	09.10.1975	42	AML (FLT3-ITD)	M1	85	46,XX	NPM1+, FLT3-ITD+
20	f	25.10.1964	53	AML (FLT3-ITD)	M4	35	46,XX	NPM1+, FLT3-ITD+
21	m	09.10.1956	62	AML (FLT3-ITD)	M2	85	46,XY	NPM1+, FLT3-ITD+
23	f	29.08.1948	65	Lymphoma	n.a.	1	46,XX	n.a.
24	m	14.06.1981	34	Lymphoma	n.a.	<1	n.a.	n.a.
25	m	19.12.1976	39	Lymphoma	n.a.	1	n.a.	none
26	m	14.07.1940	79	Lymphoma	n.a.	0	n.a.	none

Figure S1

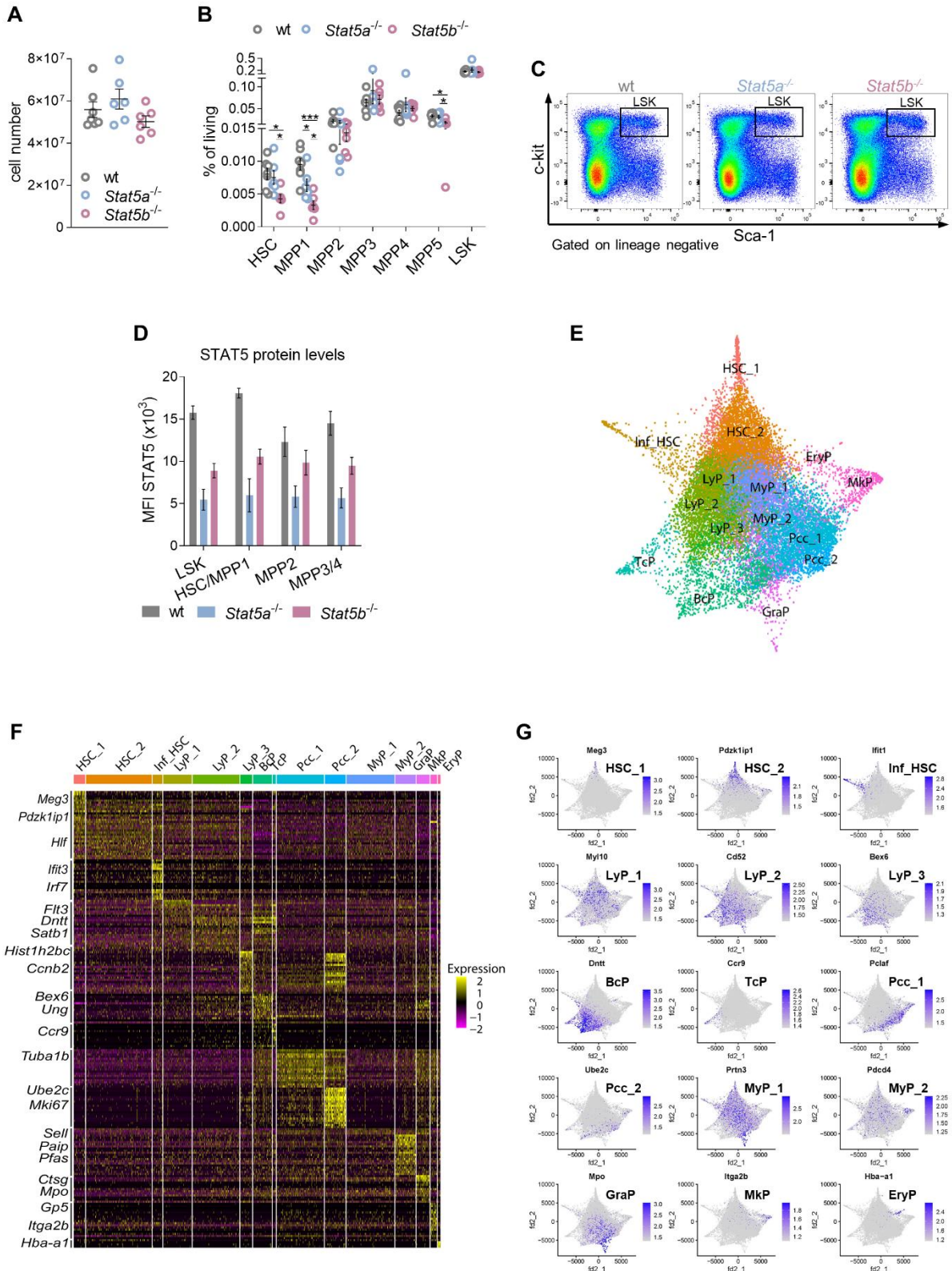


Figure S1

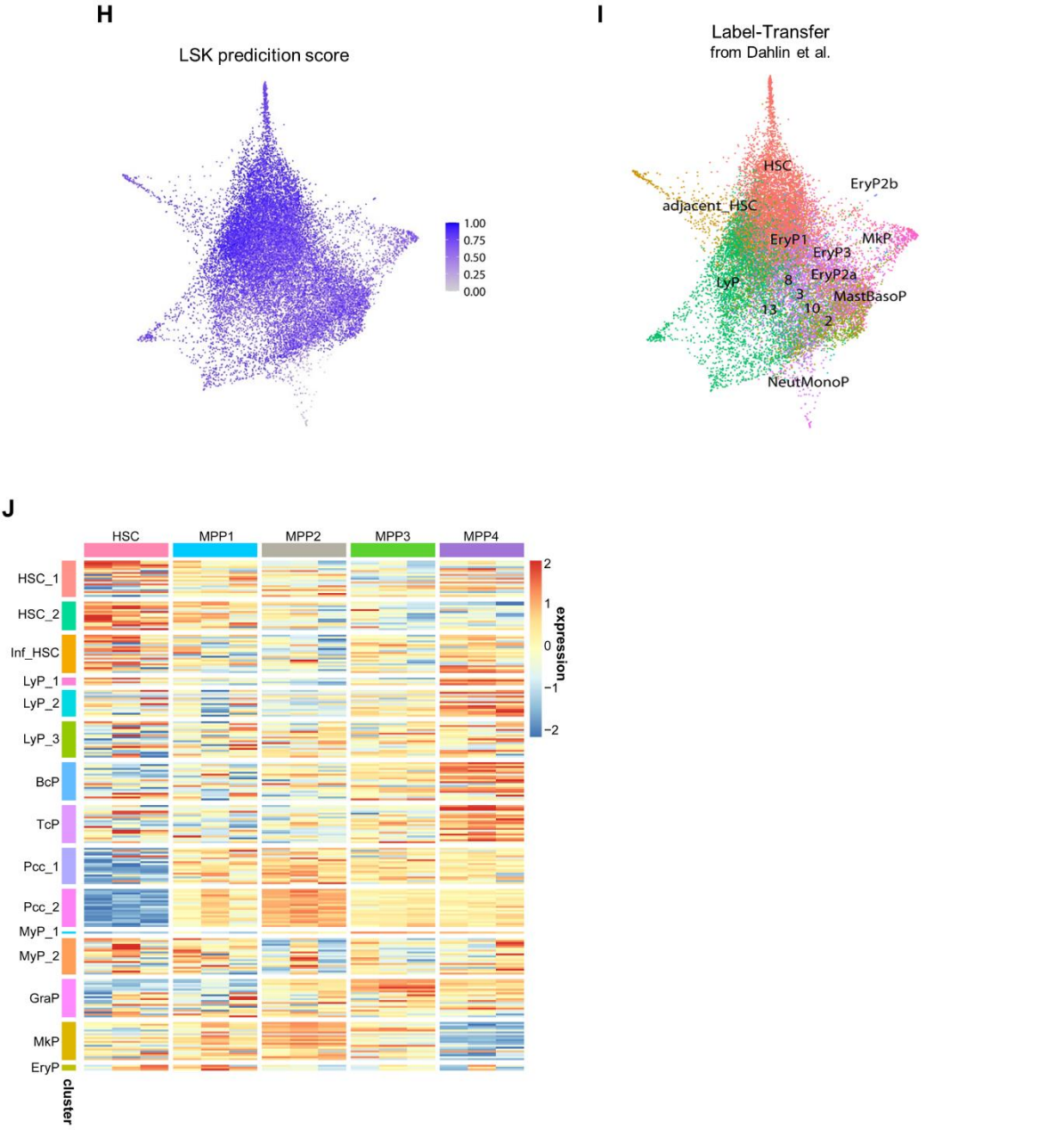
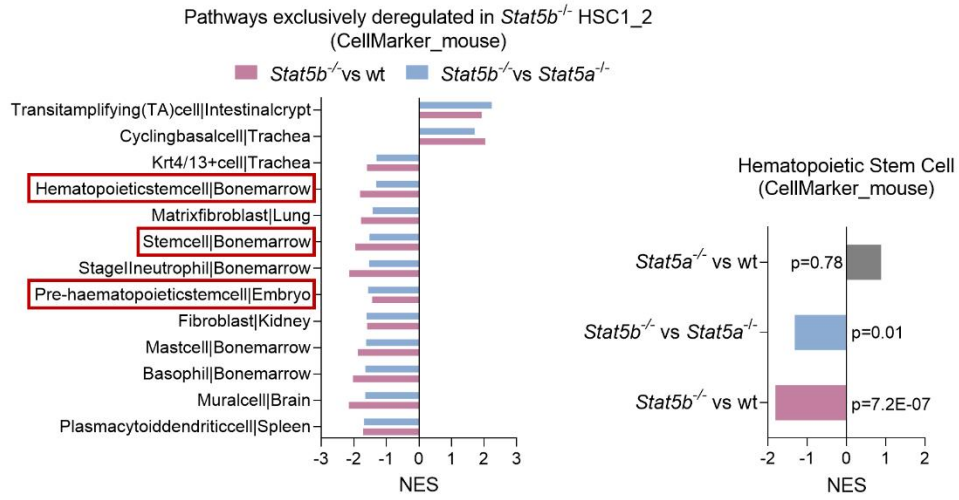


Figure S1

K



L

Molecular cell cycle score of HSC_1 and HSC_2

%	wt	<i>Stat5a</i> ^{-/-}	<i>Stat5b</i> ^{-/-}
G ₀ /G ₁	94.20	93.68	91.06
S	2.90	4.36	3.52
G ₂ M	2.90	1.96	5.42

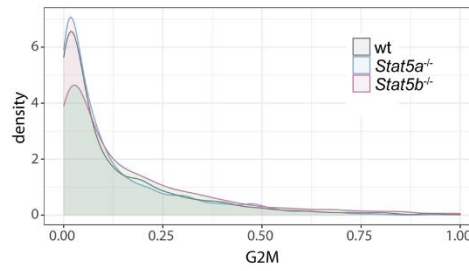


Figure S1: STAT5B, but not STAT5A, has an important role in HSC dormancy.

(A)-(B) FACS analyses of wt, *Stat5a*^{-/-} or *Stat5b*^{-/-} BM. Quantification of (A) total cell numbers (n≥6/genotype, mean±SEM) and (B) relative HSC, MPP1-5 and LSK cell numbers (n≥6/genotype, mean±SEM) and (C) representative gatings of LSK population on lineage negative cells.

(D) STAT5 levels in wt, *Stat5a*^{-/-} and *Stat5b*^{-/-} LSK, HSC/MPP1, MPP2 and MPP3/4 cells determined by flow cytometry (n=5/genotype, mean±SEM).

(E-L) Single cell RNA-seq of LSK cells from wt, *Stat5a*^{-/-} and *Stat5b*^{-/-} mice (n=3 pooled/genotype). (E) Force-directed graph showing all defined and annotated clusters. HSC_1-2: Hematopoietic stem cells_1-2, Inf_HSC: Interferon activated HSCs, LyP_1-3: Lymphoid progenitors_1-3, BcP_B-cell progenitors, TcP: T-cell progenitors, Pcc_1-2: Progenitors in cell cycle_1-2, MyP_1-2: Myeloid progenitors_1-2. GraP: Granulocyte progenitors, MkP: Megakaryocyte progenitors, EryP: Erythroid progenitors. (F) Heatmap illustrating the top 20 upregulated genes of each cluster, color code indicates z-scores. (G) Force-directed graphs with color key indicating log normalised gene expression for one representative marker gene of each defined cluster. Marker genes were chosen based on¹⁸⁻²¹. (H) Force-directed graph showing an LSK prediction score (based on¹³) for each cell in our data. Cells with a score >0.5 are predicted to be LSKs. (I) Force-directed graph showing all the transferred labels from¹³. HSC: Hematopoietic stem cells, LyP: Lymphoid progenitors, NeutMonoP: Neutrophil, granulocyte and monocyte progenitors, MastBasoP: Mast cell and basophil progenitors, EryP: Erythroid progenitors 1-3, MkP: Megakaryocyte progenitors. 92% of our HSC_1 cells and 84% of our HSC_2 cells received the label “HSC”, while 90% of our Inf_HSC cells received the label “adjacent_HSC”. 71% of our BcPs and 99% of our TcPs were labelled LyP. Cells with the strongest MkP, EryP and GraP expression profiles received MkP, EryP2b, and NeutMonoP labels. (J) Expression levels of the top (p-value < 1E-10) cluster specific genes on an independent RNA-Seq dataset of FACS-sorted HSC, MPP1, MPP2, MPP3 or MPP4 cell populations from Cabezas-Wallscheid et al.¹⁸. (K) GSEA (Gene Set Enrichment Analysis) of HSC_1 and HSC_2 cells using the CellMarker database²². NES: Normalized Enrichment Score (L) Molecular cell cycle score. (*Left*) Percentages of cells predicted to be in G₀/G₁, S and G₂M phase in pooled HSC_1 and HSC_2 clusters and (*right*) density plots of the G₂M score of each genotype.

Levels of significance were calculated using 1-way ANOVA in (B) and unpaired t-test in (K) *p < 0.05, ***p < 0.001.

Figure S2

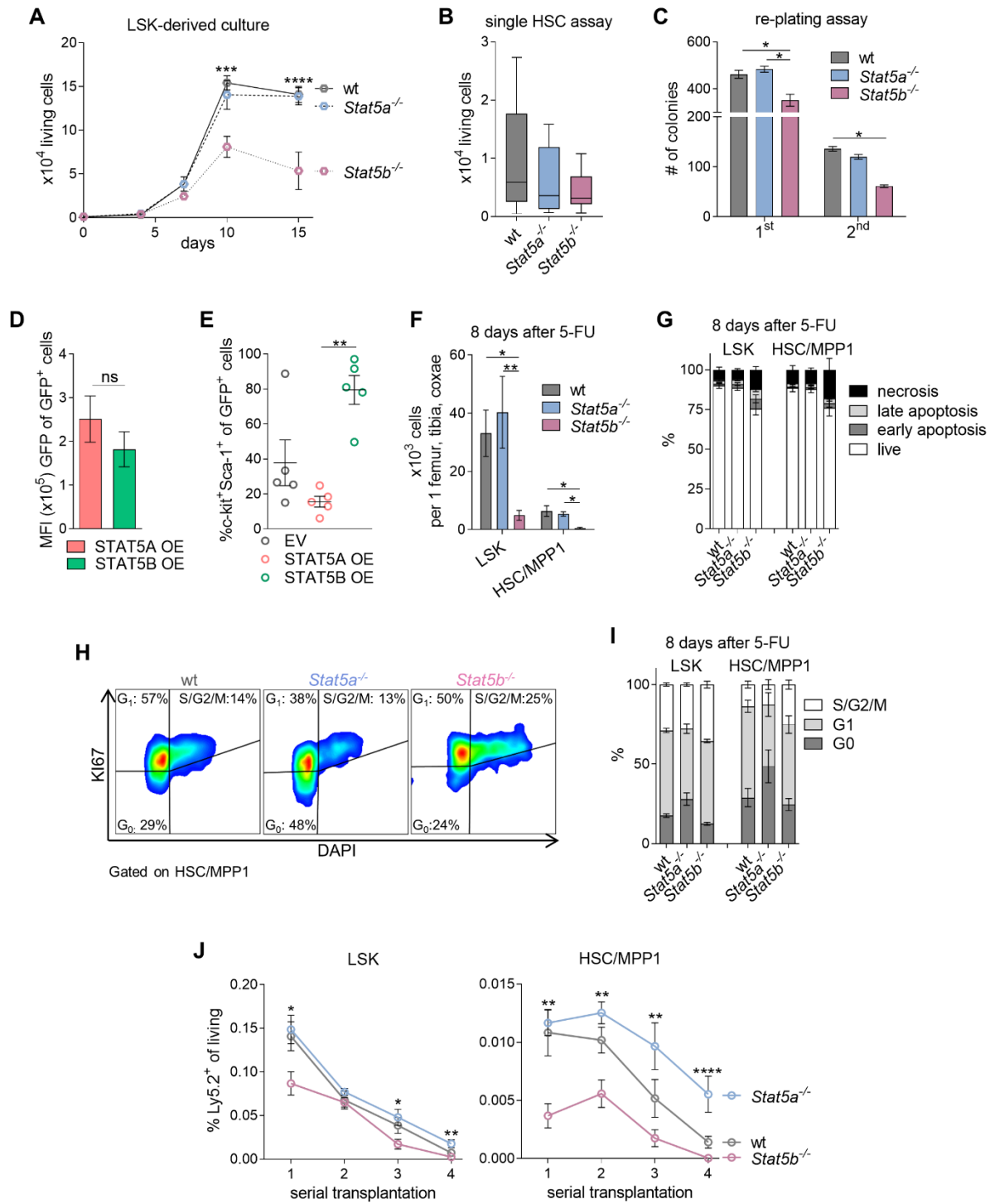


Figure S2: STAT5B drives HSC self-renewal.

(A) *Ex vivo* growth analysis of LSK cells of wt, *Stat5a*^{-/-} and *Stat5b*^{-/-} BM. 5x10³ LSK cells were FACS-sorted, cultured and counted over 15 days (n=3/genotype, mean±SEM).

(B) Single HSC assay using cell surface markers (Lineage⁻ (CD3, CD19, CD11b, Gr-1, Ter-119), c-kit⁺, Sca-1⁺, CD150⁺, CD48⁻). wt, *Stat5a*^{-/-} or *Stat5b*^{-/-} BM: total cell numbers derived from a single HSC/MPP1 cell after 10 days (n=74/genotype, whiskers: Tukey).

(C) Colony numbers of serial plating of FACS-sorted LSK cells of wt, *Stat5a*^{-/-} and *Stat5b*^{-/-} BM (n=3/genotype, mean±SEM).

(D)-(E) STAT5A (STAT5A-GFP) or STAT5B (STAT5B-GFP) over-expression in LSK cells. EV (empty vector-GFP) was used as control. (D) GFP levels of LSK cells expressing STAT5A-GFP or STAT5B-GFP (n=5/genotype, mean±SEM). (E) Quantification of c-kit and Sca-1 expression on GFP⁺ cells (n=5/genotype, mean±SEM).

(F)-(I) 5-FU recovery assays of wt, *Stat5a*^{-/-} or *Stat5b*^{-/-} mice. Mice were analysed 8-days after 5-FU injection. (F) Quantification of LSK and HSC/MPP1 cell numbers (n=5/genotype, mean±SEM). (G) Annexin-V/DAPI staining of LSK and HSC/MPP1 cells showing distribution of live (Annexin-V⁻/DAPI⁻), necrotic (Annexin-V⁻/DAPI⁺), early apoptotic (Annexin-V⁺/DAPI⁻) and late apoptotic (Annexin-V⁺/DAPI⁺) cells (n=5/genotype, mean±SEM). (H) Representative FACS plots and gating strategy of cell cycle analysis (KI67/DAPI) of HSC/MPP1 cells and (I) the cell cycle phase distribution of LSK and HSC/MPP1 cells (n=5/genotype, mean±SEM).

(J) Serial transplantation assays of wt, *Stat5a*^{-/-} or *Stat5b*^{-/-} BM cells. 5x10⁶ BM cells (Ly5.2⁺) were injected in lethally Ly5.1⁺ irradiated recipient mice and reinjected 8 weeks thereafter. Quantification of (*left*) Ly5.2⁺ LSK cells (n=5/genotype, mean±SEM) and (*right*) Ly5.2⁺ HSC/MPP1 cells in recipient mice in primary, secondary, tertiary and quaternary transplantation (n=5/genotype, mean±SEM).

Levels of significance were calculated using 1-way ANOVA in (C), (E), (F), (J) and using 2-way ANOVA in (A) and using Wilcoxon test in (D). *p < 0.05, **p < 0.01, ***p < 0.001, and ****p < 0.0001.

Figure S3

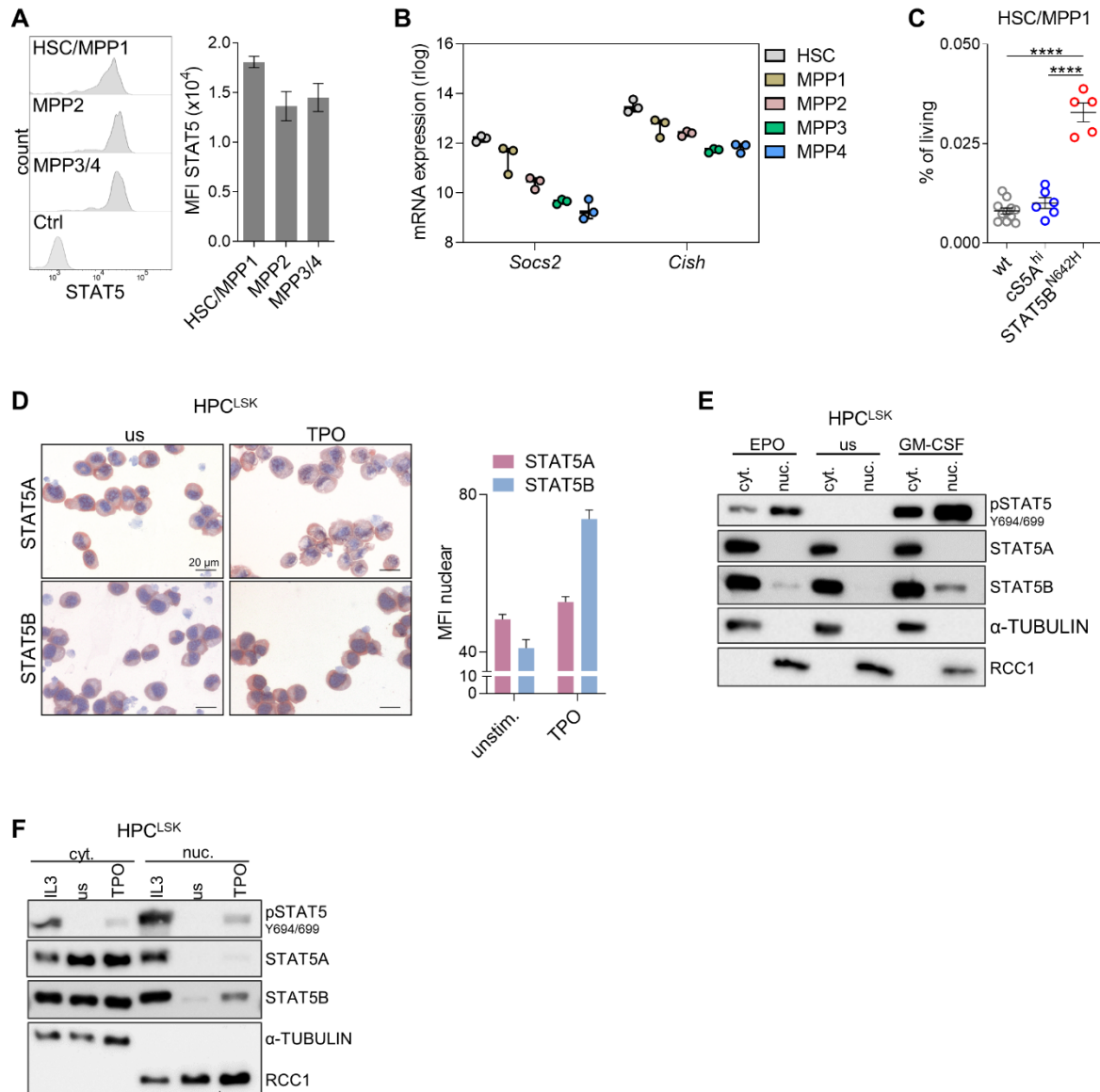


Figure S3: Selective STAT5B activation in HSCs drives self-renewal.

(A)-(B) Analysis of STAT5 signaling in HSC subpopulations. (A) (*Left*) Representative histograms of STAT5 MFI levels of wt HSC/MPP1, MPP2 and MPP3/4 cells and isotype control (Ctrl) and (*right*) the quantification of STAT5 levels. (B) *Socs2* and *Cish* rlog transformed mRNA expression of FACS-sorted murine HSC and MPP1-4 subpopulations (analysis of published data¹⁸).

(C) Relative quantification of HSC/MPP1 cells expressing hyperactive STAT5A (cS5A^{hi}) or STAT5B (STAT5B^{N642H}) isolated from BM of transgenic mice (n≥5/genotype, mean±SEM).

(D) (*Left*) STAT5A or STAT5B IHC staining of HPC^{LSK} wt cytopins with or without 20 min TPO stimulation. Scale bar indicates 20 μm. Representative pictures of three independent experiments. (*Right*) Quantification of nuclear STAT5A and STAT5B MFI levels. Quantification of three pictures of one out of four independent HPC^{LSK} cell lines.

(E)-(F) pSTAT5 (Y694/699), STAT5A, and STAT5B immunoblot analysis of cytoplasmic and nuclear fractions of HPC^{LSK} wt cells after 20 min stimulation with (D) EPO or GM-CSF, or (E) IL3 or TPO stimulation or without stimulation (us). RCC1 is used as loading control for the nuclear, α-TUBULIN for the cytoplasmic fraction.

Levels of significance were calculated using 1-way ANOVA in (C). ****p < 0.0001.

Figure S4

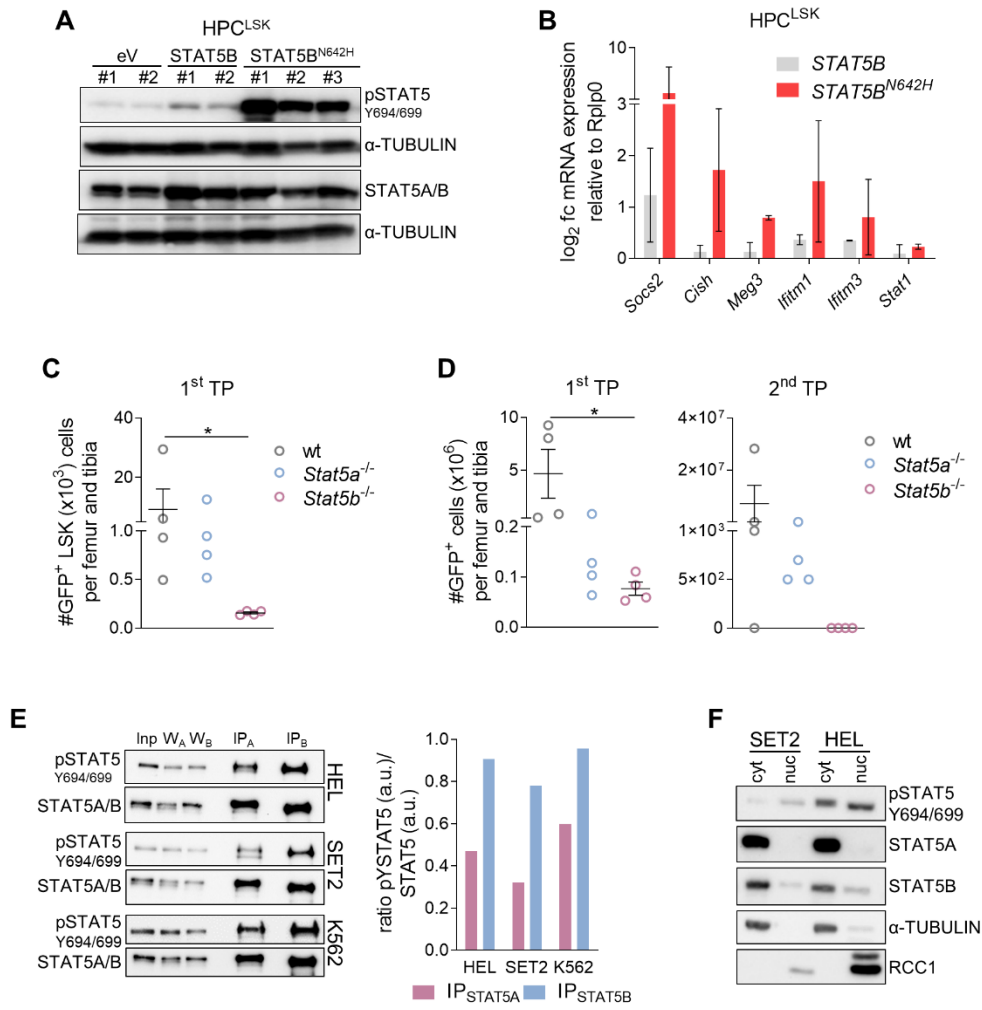


Figure S4: Selective STAT5B activation drives the self-renewal of LSCs.

(A)-(B) Analysis of HPC^{LSK} cells expressing empty Vector (eV), STAT5B or STAT5B^{N642H}. (A) pSTAT5 (Y694/699), STAT5A/B and α -TUBULIN (loading control) immunoblot analysis and (B) quantification of mRNA expression (n=3/genotype, mean \pm SEM).

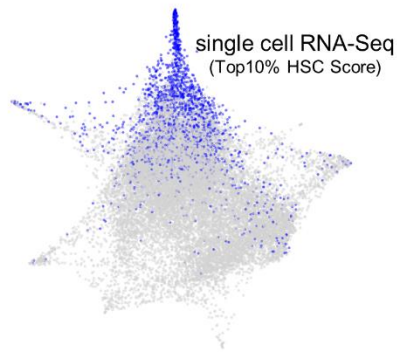
(C)-(D) BCR/ABL^{p210-GFP+} LSK re-transplantation assay. (C) BCR/ABL^{p210-GFP+} LSK cell numbers in recipients' BM 13 weeks after 1st transplantation (TP, n=4/genotype, mean \pm SEM) and (D) BCR/ABL^{p210-GFP+} cell numbers after 1st and 2nd TP (n=4/genotype, mean \pm SEM).

(E)-(F) Analysis of pYSTAT5 levels in the presence of oncoproteins. Input (Inp), W_A (wash fraction of STAT5A IP), W_B (wash fraction of STAT5B IP), IP (immunoprecipitate). (E) *Left*: pSTAT5 (Y694/699) and STAT5A/B immunoblot analysis of IP of either STAT5A or STAT5B of human HEL (JAK2^{V617F}), SET2 (JAK2^{V617F}) and K562 (BCR/ABL1) leukemic cell lines and (*right*) their quantification. (F) pSTAT5 (Y694/699), STAT5A and STAT5B immunoblots of cytoplasmic and nuclear fractions isolated from HEL and SET2 cell lines. RCC1 is used as loading control for the nuclear, α -TUBULIN for the cytoplasmic fraction. Representative blots of three independent experiments are shown.

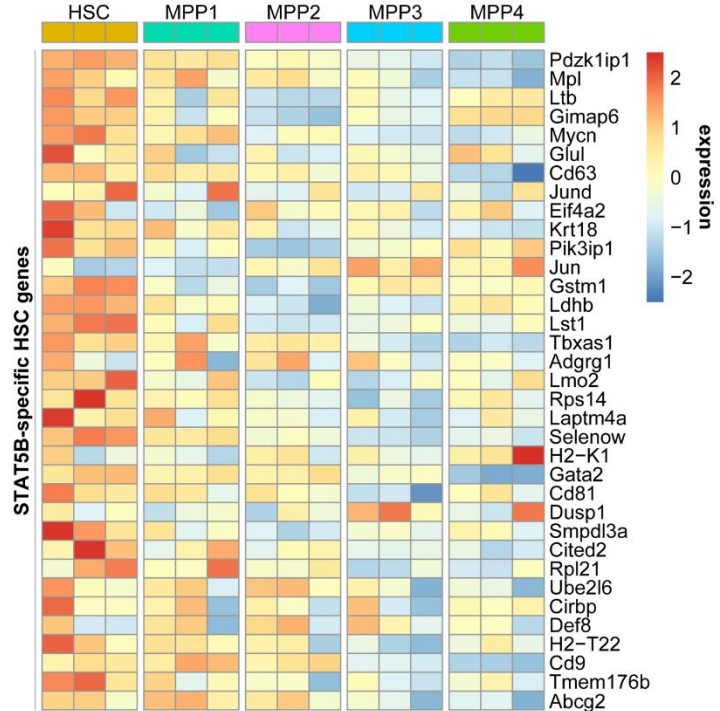
Levels of significance were calculated using 1-way ANOVA in (C) and (D). *p < 0.05.

Figure S5

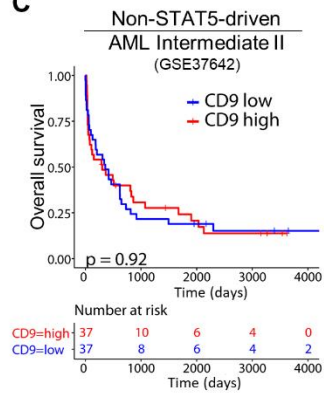
A



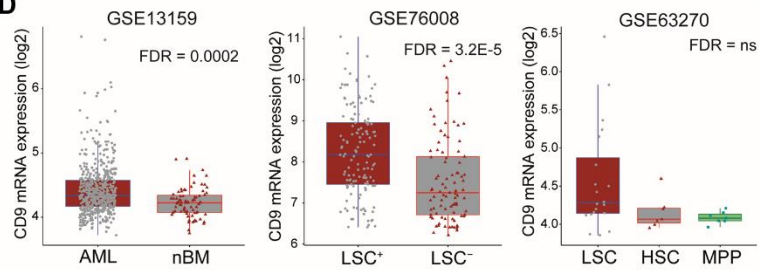
B



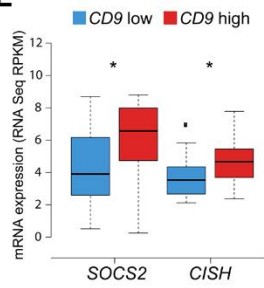
C



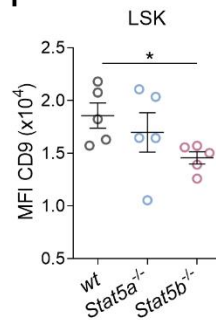
D



E



F



G

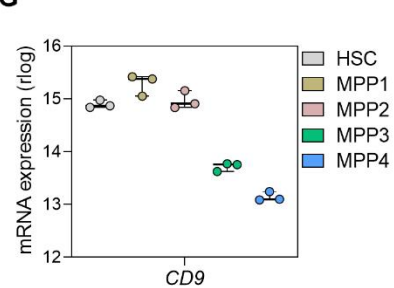


Figure S5

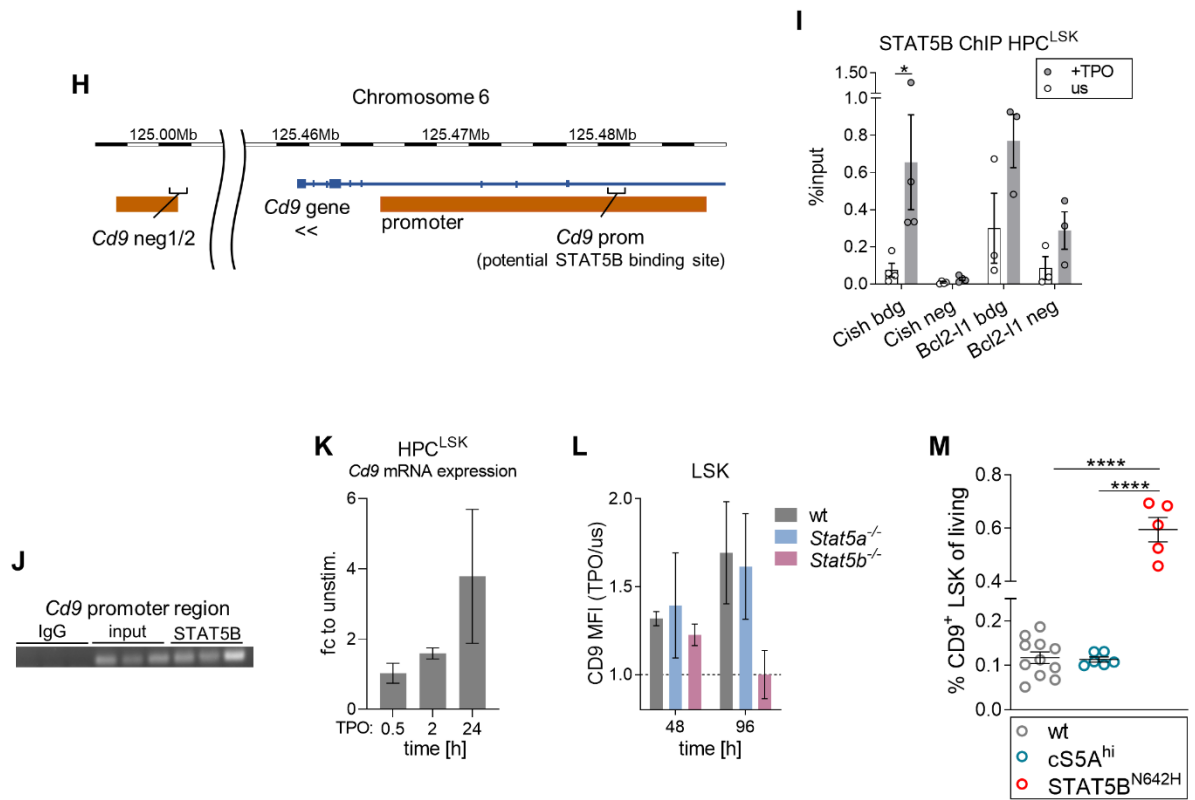


Figure S5: CD9 as marker and direct target of pYSTAT5B signaling.

(A) Literature-defined HSC score analysed in wt, *Stat5a*^{-/-} and *Stat5b*^{-/-} single cell RNA-seq data, force-directed graph illustrating the top 10% cells with the highest HSC score.

(B) Expression of the STAT5B-specific HSC genes on an independent RNA-Seq dataset of FACS-sorted HSC, MPP1, MPP2, MPP3 or MPP4 cell populations from Cabezas-Wallscheid et al.¹⁸

(C) Survival analysis comparing *CD9*-low vs. *CD9*-high expressing patients in non-STAT5-driven cohort GSE37642 (Intermediate II).

(D) Comparison of *CD9* mRNA expression in (*left*) AML (n=542) and nBM (n=74; normal BM, GSE13159), (*middle*) LSC⁻ (n=89) and LSC⁺ (n=138; GSE76008) and (*right*) LSC (n=20), HSC (n=7) and MPP (n=7; GSE63270).

(E) *SOCS2* and *CISH* mRNA expression in *CD9*-low and *CD9*-high expressing FLT3-mut. NPM1-mut. patients (OHSU) (n=45).

(F) Flow cytometry analysis of CD9 surface levels on wt, *Stat5a*^{-/-} and *Stat5b*^{-/-} LSK cells (n=5/genotype, mean±SEM).

(G) *Cd9* rlog transformed mRNA expression levels on an independent RNA-Seq dataset of FACS-sorted HSC, MPP1, MPP2, MPP3 or MPP4 cell populations from Cabezas-Wallscheid et al.¹⁸

(H)-(J) STAT5B ChIP-qPCR in HPC^{LSK} wt cells with or without 30 min TPO stimulation. (H) Schematic overview of the *Cd9* promoter indicating the primer binding sites designed for *Cd9* promoter (*Cd9* prom) and *Cd9* negative regions 1 and 2 (*Cd9* neg1/2). (I) Quantification of STAT5B binding to the *Cish* and *Bcl2l1* promoter (*bdg*) or negative regions (*neg*) in HPC^{LSK} wt cells with or without TPO stimulation (n≥3/condition, mean±SEM). (J) Gel electrophoresis of the *Cd9* promoter PCR product. IgG: IgG antibody ChIP was performed as control.

(K) *Cd9* mRNA expression of HPC^{LSK} wt cells 0.5, 2 and 24 h after TPO stimulation relative to unstimulated (fc – fold change, n=2/condition, mean±SEM).

(L) CD9 surface levels of wt, *Stat5a*^{-/-} and *Stat5b*^{-/-} *ex vivo* LSK cells cultured for 48 and 96 h with TPO relative to unstimulated (n=2/genotype and condition, mean±SEM).

(M) Relative quantification of CD9 expressing LSK cells of wt, cS5A^{hi} and STAT5B^{N642H} mice (n≥5/genotype, mean±SEM).

Levels of significance were calculated using log rank test in (C), unpaired t-test for *CISH* and Mann-Whitney for *SOCS2* in (E), 1-way ANOVA in (F), (M) and paired t-test in (I). False discovery rates (FDR) in (D) were calculated using the *lmfit* function of the *limma* package. *p < 0.05 and ****p < 0.0001.

Figure S6

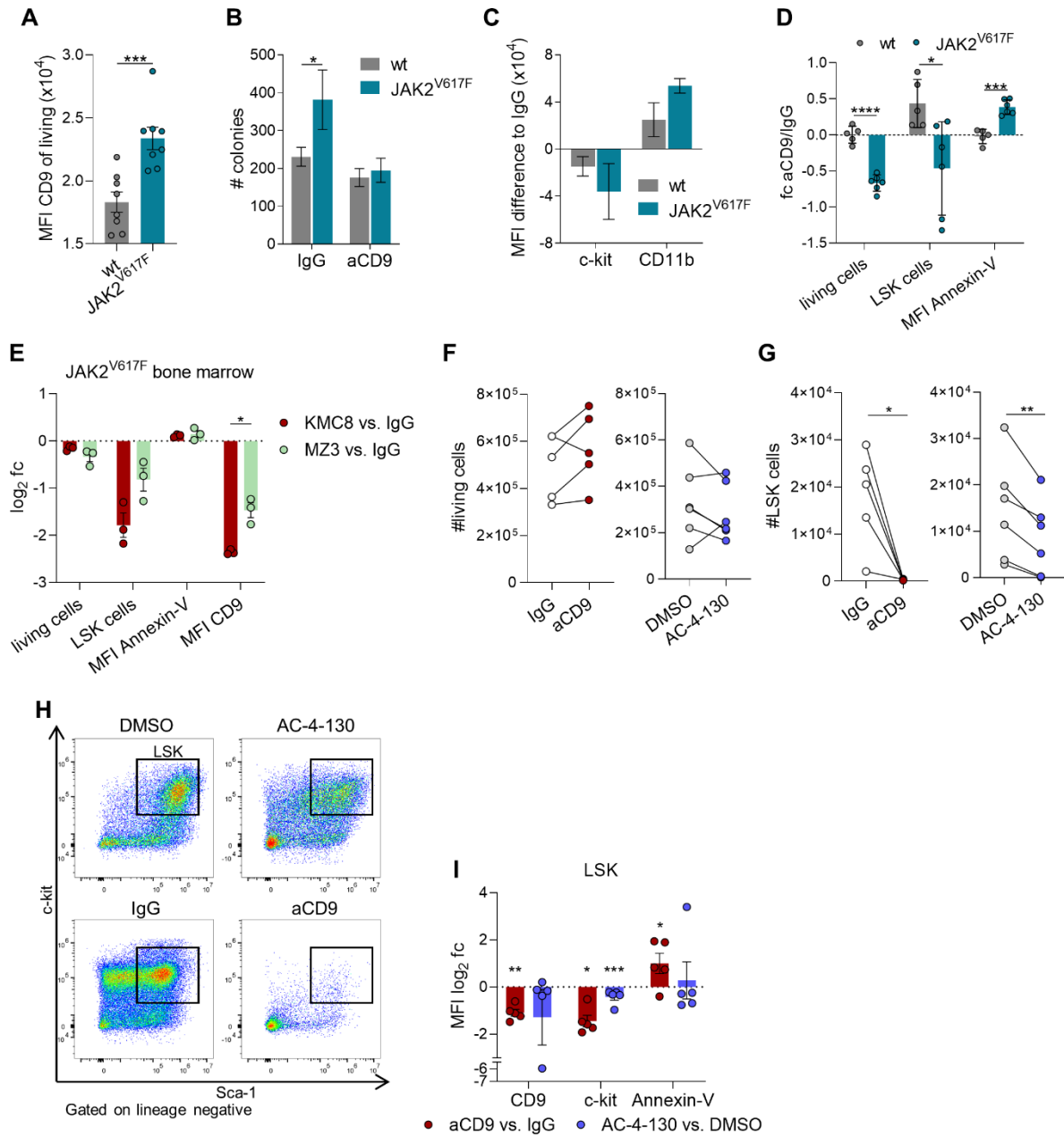


Figure S6: CD9 blocking affects STAT5 activation and impedes self-renewal.

(A) CD9 surface levels on wt and JAK2^{V617F} BM cells (n=8/genotype, mean±SEM) determined by flow cytometry.

(B)-(C) Colony formation assays of wt and JAK2^{V617F} BM cells either treated with IgG or aCD9 (5 µg/ml). (B) Colony numbers (n≥3/genotype and condition, mean±SEM) and (C) c-kit and CD11b expression levels (n=3/genotype and condition, mean±SEM).

(D) *In vitro* treatment of wt and JAK2^{V617F} BM either with IgG or aCD9. Ratio of aCD9/IgG of Annexin-V levels, living and LSK cell numbers (n≥5/genotype and condition, mean±SEM).

(E) *In vitro* treatment of JAK2^{V617F} BM either with IgG, aCD9 (KMC8) or aCD9 (MZ3) for 96h. Log₂ fc of aCD9/IgG of number of living or LSK cells and MFI of Annexin-V and CD9 levels (n=3/genotype and condition, mean±SEM).

(F)-(I) Comparison of 96 h treatment with AC-4-130 (5 µM, DMSO was used as control) to aCD9 (5 µg/ml, IgG was used as control) of JAK2^{V617F} BM cells. (F) Total cell numbers of treated cells. (G) Total LSK cell numbers of treated cells. (H) Representative flow cytometry dot plots of treated LSK cells. (I) Log₂ fc of CD9, c-kit, or AnnexinV MFI levels of aCD9- or AC-4-130 treated cells compared to the respective control (n≥5/condition, mean±SEM).

Fold change (fc). Levels of significance were calculated using unpaired t-test in (A), (B) and (D) and paired t-test in (E), (G) and (I). *p < 0.05, **p < 0.01, ***p < 0.001, and ****p < 0.0001.

Figure S7

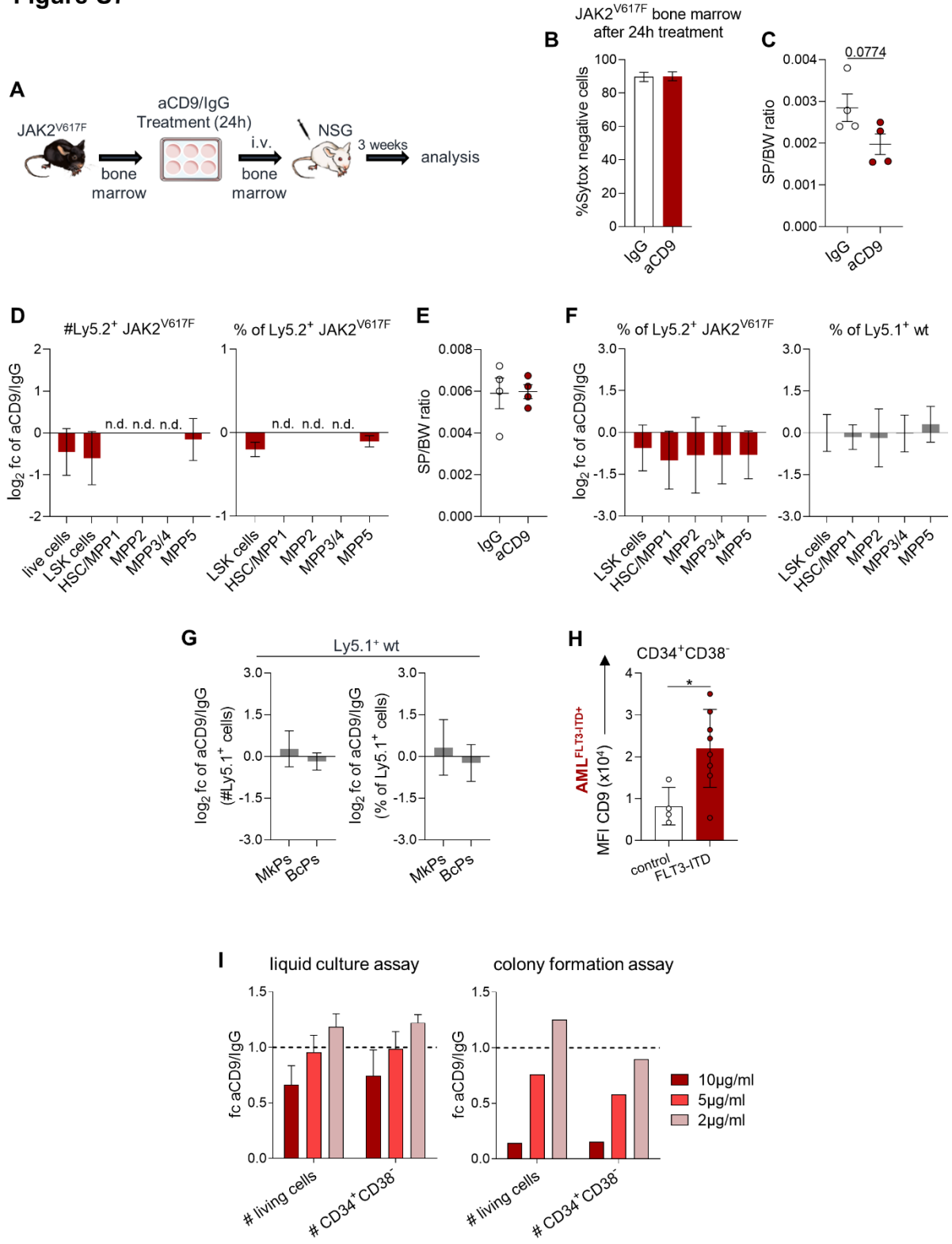


Figure S7

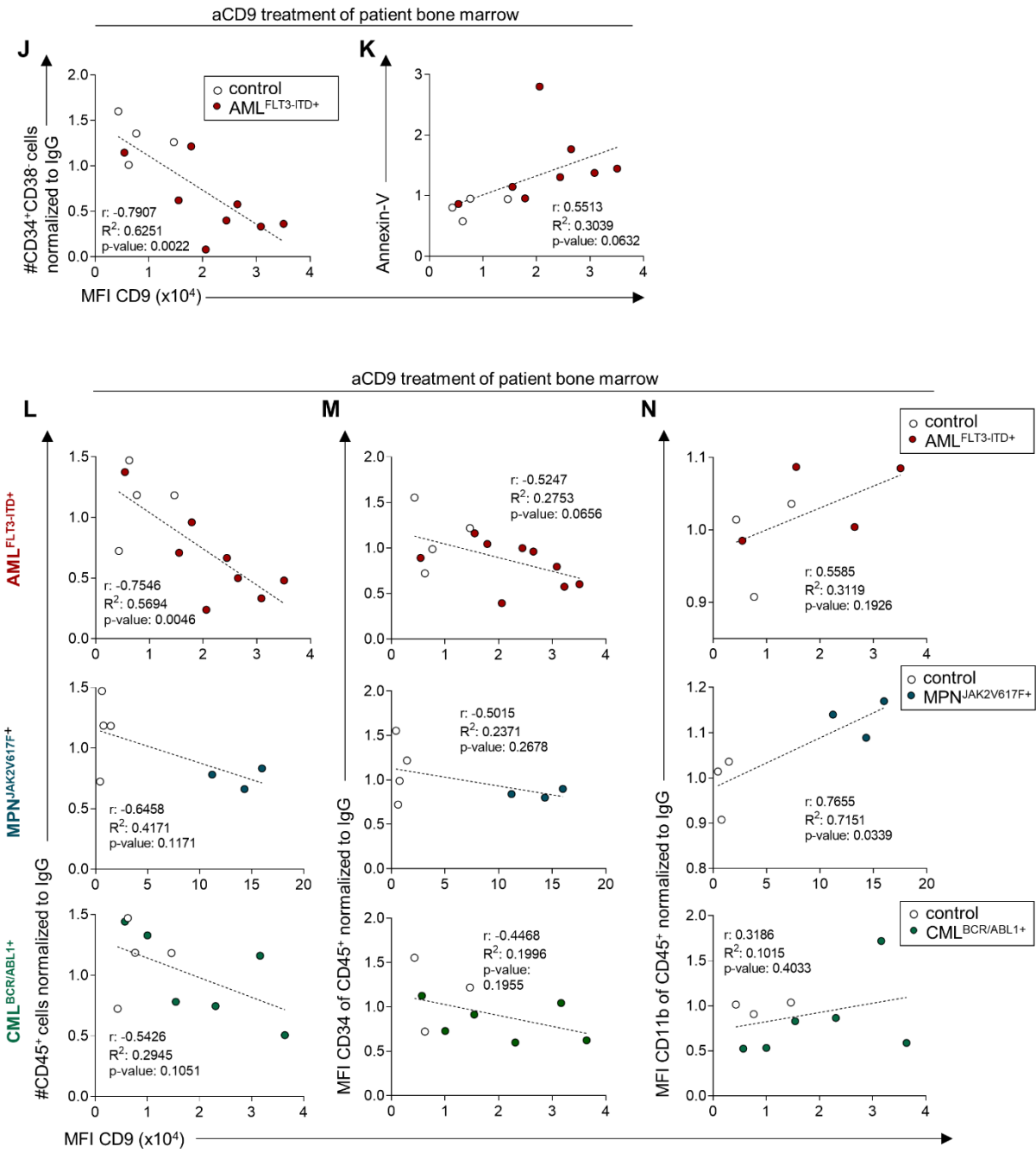


Figure S7

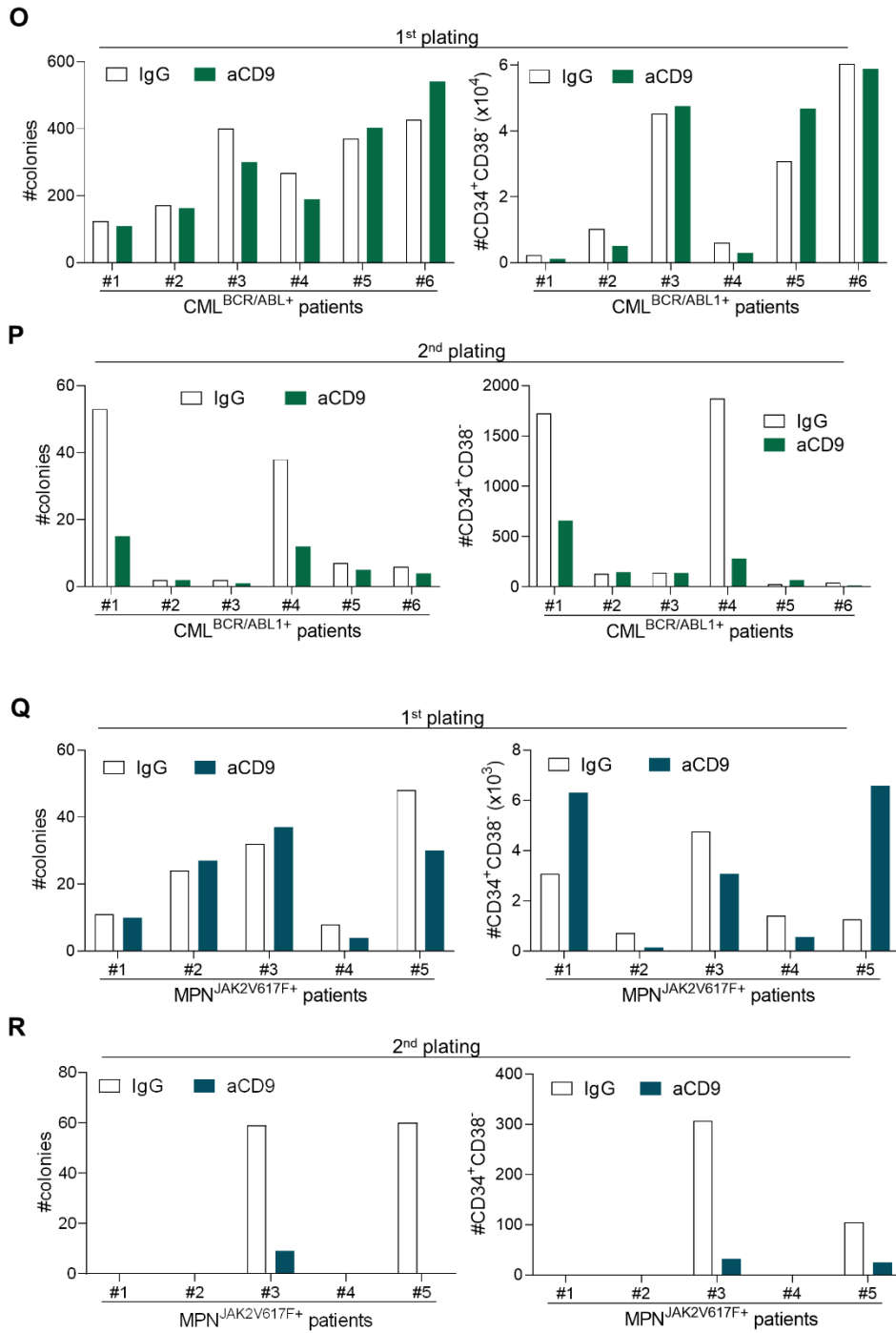


Figure S7: CD9 as a therapeutic target for pYSTAT5-driven leukemia.

(A)-(D) JAK2^{V617F} transplantation with aCD9 pre-treatment. (A) Experimental workflow. (B) Viability of IgG or aCD9 treated JAK2^{V617F} BM cells prior transplantation determined by Sytox staining. (C) Spleen (SP) relative to body weight of NSG recipient mice. (D) Fold changes (aCD9 vs IgG) of Ly5.2⁺ JAK2^{V617F} donor (*left*) HSC subpopulations and total BM cell numbers and (*right*) HSC subpopulations % of Ly5.2⁺ cells (n=4/treatment, mean±SEM). Not determined (n.d.).

(E)-(G) JAK2^{V617F} transplantation with aCD9 *in vivo* treatment. (E) SP sizes relative to body weight of NSG recipient mice. (F) Log₂ fold changes (aCD9 vs IgG) of HSC/subpopulations % of Ly5.2⁺ cells of (*left*) Ly5.2⁺ JAK2^{V617F} donor or (*right*) Ly5.1⁺ wt NSG recipient cells. (G) Log₂ fold changes (aCD9 vs IgG) of megakaryocyte progenitor (MkPs, Lin⁻ c-kit⁺ Sca-1⁻ CD150⁺ CD41⁺) and early B-cell progenitor (BcPs, Lin⁻ cKit^{mid} CD93⁺ CD127⁺ CD19⁻) (*left*) total cell numbers and (*right*) % of Ly5.2⁺ and Ly5.1⁺ cells (n=4/treatment, mean±SEM, 4x 1.25 mg/kg i.v. IgG or aCD9 were applied).

(H) Analysis of CD9 levels on CD34⁺CD38⁻ cells of AML^{FLT3-ITD} (n=8) and control (n=4) BM.

(I) aCD9 dosage to achieve non-toxic condition in human patient BM samples. Fold change (aCD9 relative to IgG) of CD34⁺CD38⁻ and total cell numbers in (*left*) 2-day liquid culture and (*right*) CFA using different aCD9 concentrations.

(J)-(K) *In vitro* treatment of control and patient BM cells either treated with IgG or aCD9 (2 µg/ml). XY plots showing CD9 levels and (J) CD34⁺CD38⁻ cell numbers or (K) Annexin-V levels of control (n=4) and AML^{FLT3-ITD+} (n=8) patient BM MNCs.

(L)-(N) *In vitro* treatment of control and patient BM either with IgG or aCD9 (2 µg/ml). XY plots showing CD9 levels and (L) CD45⁺ cell numbers, (M) CD34 levels or (N) CD11b levels of control (n=4) in (*top*) AML^{FLT3-ITD+} (n=8), (*middle*) MPN^{JAK2V617F+} (n=3) and (*bottom*) CML^{BCR/ABL1+} (n=6) patient BM.

(O)-(P) Serial plating assays of CML^{BCR/ABL1+} (n=6) patient BM either treated with IgG or aCD9. Quantification of (*left*) colony and (*right*) CD34⁺CD38⁻ cell numbers after the (O) primary and (P) secondary plating.

(Q)-(R) Serial plating assays of MPN^{JAK2V617F+} (n=5) patient BM either treated with IgG or aCD9. Quantification of (*left*) colony and (*right*) CD34⁺CD38⁻ cell numbers after the (Q) primary and (R) secondary plating.

Levels of significance were calculated using unpaired t-test in (C) and (H). Levels of significance and correlation were calculated using Pearson in (J)-(N).

1 Supplementary References

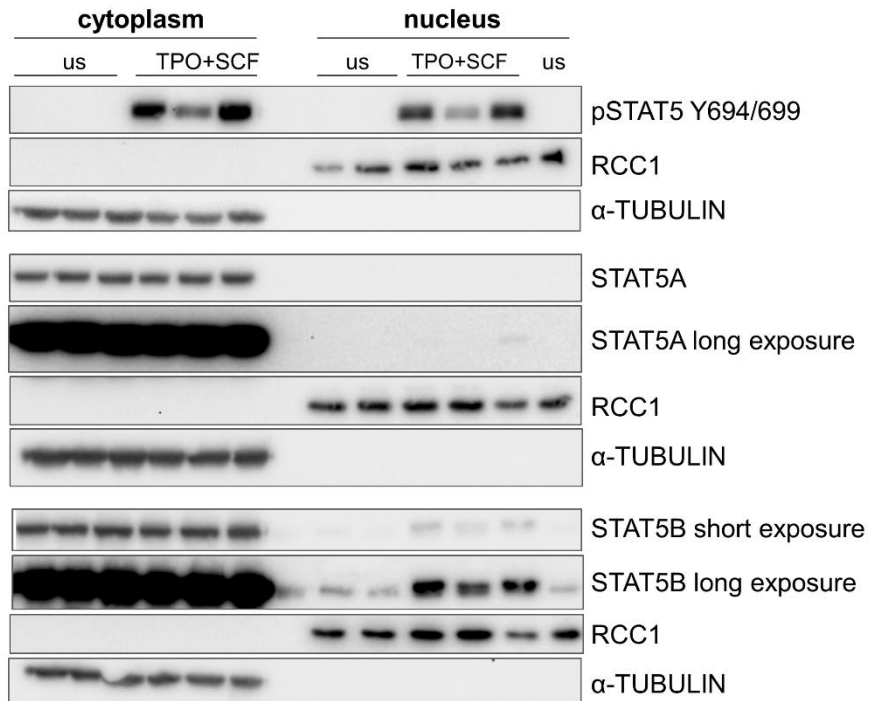
- 2 1. Doma E, Mayer IM, Brandstoetter T, et al. A robust approach for the generation of functional hematopoietic
3 progenitor cell lines to model leukemic transformation. *Blood Adv.* 2021;5(1):39–53.
- 4 2. Pinto Do Ó P, Kolterud Å, Carlsson L. Expression of the LIM-homeobox gene LH2 generates immortalized Steel
5 factor-dependent multipotent hematopoietic precursors. *EMBO J.* 1998;17(19):5744–5756.
- 6 3. Hoelbl A, Schuster C, Kovacic B, et al. Stat5 is indispensable for the maintenance of *bcr/abl*-positive leukaemia.
7 *EMBO Mol. Med.* 2010;2(3):98–110.
- 8 4. Galvin A, Weglarz M, Folz-Donahue K, et al. Cell Cycle Analysis of Hematopoietic Stem and Progenitor Cells
9 by Multicolor Flow Cytometry. *Curr. Protoc. Cytom.* 2019;87(1):e50.
- 10 5. Berger A, Hoelbl-Kovacic A, Bourgeais J, et al. PAK-dependent STAT5 serine phosphorylation is required for
11 BCR-ABL-induced leukemogenesis. *Leukemia.* 2014;28(3):629–641.
- 12 6. Schmidt L, Heyes E, Scheiblecker L, et al. CEBPA-mutated leukemia is sensitive to genetic and pharmacological
13 targeting of the MLL1 complex. *Leukemia.* 2019;33(7):1608–1619.
- 14 7. Maurer B, Nivarthi H, Wingelhofer B, et al. High activation of STAT5A drives peripheral T-cell lymphoma and
15 leukemia. *Haematologica.* 2020;105(2):435–447.
- 16 8. Warsch W, Grundschober E, Berger A, et al. STAT5 triggers BCR-ABL1 mutation by mediating ROS production
17 in chronic myeloid leukaemia. *Oncotarget.* 2012;3(12):1669–87.
- 18 9. Wingelhofer B, Maurer B, Heyes EC, et al. Pharmacologic inhibition of STAT5 in acute myeloid leukemia.
19 *Leukemia.* 2018;32(5):1135–1146.
- 20 10. Hoelbl A, Kovacic B, Kerenyi MA, et al. Clarifying the role of Stat5 in lymphoid development and Abelson-
21 induced transformation. *Blood.* 2006;107(12):4898–906.
- 22 11. Stuart T, Butler A, Hoffman P, et al. Comprehensive Integration of Single-Cell Data. *Cell.* 2019;177(7):1888-
23 1902.e21.
- 24 12. Butler A, Hoffman P, Smibert P, Papalexi E, Satija R. Integrating single-cell transcriptomic data across different
25 conditions, technologies, and species. *Nat. Biotechnol.* 2018;36(5):411–420.
- 26 13. Dahlin JS, Hamey FK, Pijuan-Sala B, et al. A single-cell hematopoietic landscape resolves 8 lineage trajectories
27 and defects in Kit mutant mice. *Blood.* 2018;131(21):e1–e11.
- 28 14. Scialdone A, Natarajan KN, Saraiva LR, et al. Computational assignment of cell-cycle stage from single-cell
29 transcriptome data. *Methods.* 2015;85:54–61.
- 30 15. Gao J, Aksoy BA, Dogrusoz U, et al. Integrative analysis of complex cancer genomics and clinical profiles using
31 the cBioPortal. *Sci. Signal.* 2013;6(269):p11.
- 32 16. McCall MN, Bolstad BM, Irizarry RA. Frozen robust multiarray analysis (fRMA). *Biostatistics.* 2010;11(2):242–
33 53.
- 34 17. Nguyen CH, Schlerka A, Grandits AM, et al. IL2RA Promotes Aggressiveness and Stem Cell-Related Properties
35 of Acute Myeloid Leukemia. *Cancer Res.* 2020;80(20):4527–4539.
- 36 18. Cabezas-Wallscheid N, Klimmeck D, Hansson J, et al. Identification of regulatory networks in HSCs and their
37 immediate progeny via integrated proteome, transcriptome, and DNA methylome analysis. *Cell Stem Cell.*
38 2014;15(4):507–522.
- 39 19. Pei W, Shang F, Wang X, et al. Resolving Fates and Single-Cell Transcriptomes of Hematopoietic Stem Cell
40 Clones by PolyloxExpress Barcoding. *Cell Stem Cell.* 2020;27(3):383-395.e8.
- 41 20. Giladi A, Paul F, Herzog Y, et al. Single-cell characterization of haematopoietic progenitors and their trajectories
42 in homeostasis and perturbed haematopoiesis. *Nat. Cell Biol.* 2018;20(7):836–846.
- 43 21. Wilson NK, Kent DG, Buettner F, et al. Combined Single-Cell Functional and Gene Expression Analysis Resolves
44 Heterogeneity within Stem Cell Populations. *Cell Stem Cell.* 2015;16(6):712–24.
- 45 22. Zhang X, Lan Y, Xu J, et al. CellMarker: A manually curated resource of cell markers in human and mouse.
46 *Nucleic Acids Res.* 2019;47(D1):D721–D728.

47

48 Annex

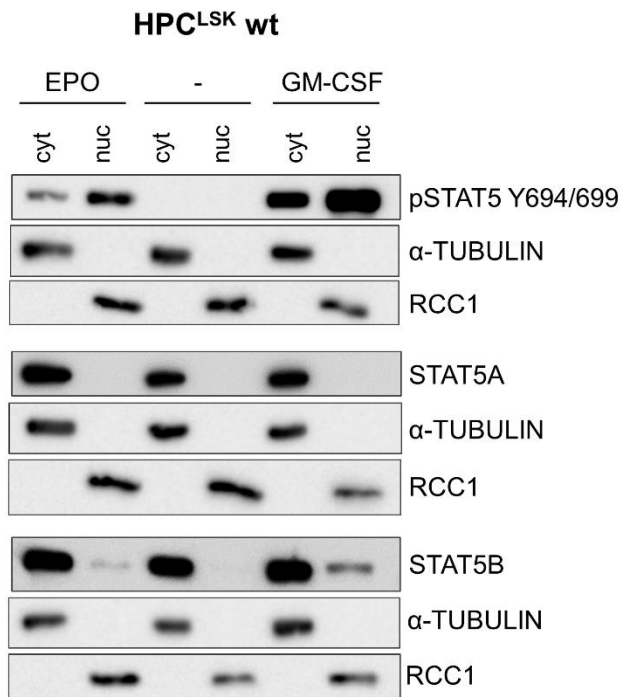
49 Part I: Cropped WB membranes including all loading controls

Figure 3E



50

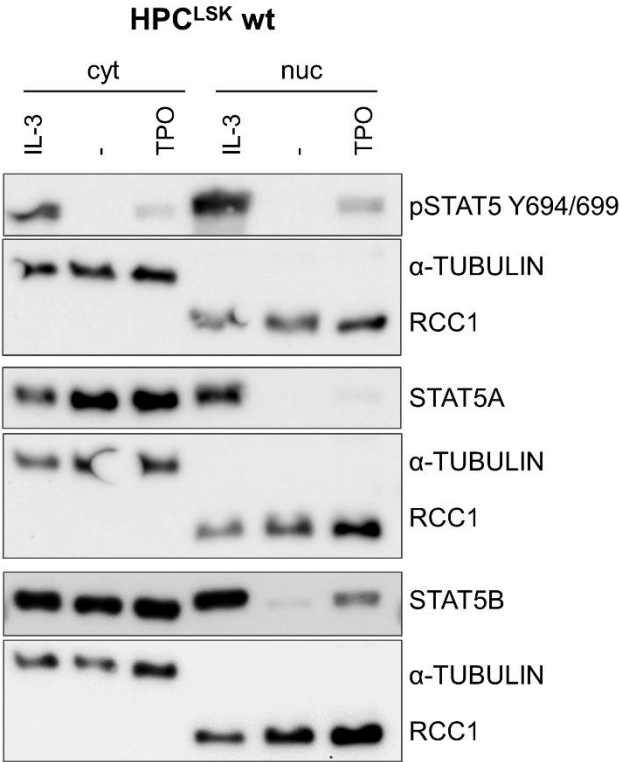
Figure S3E



51

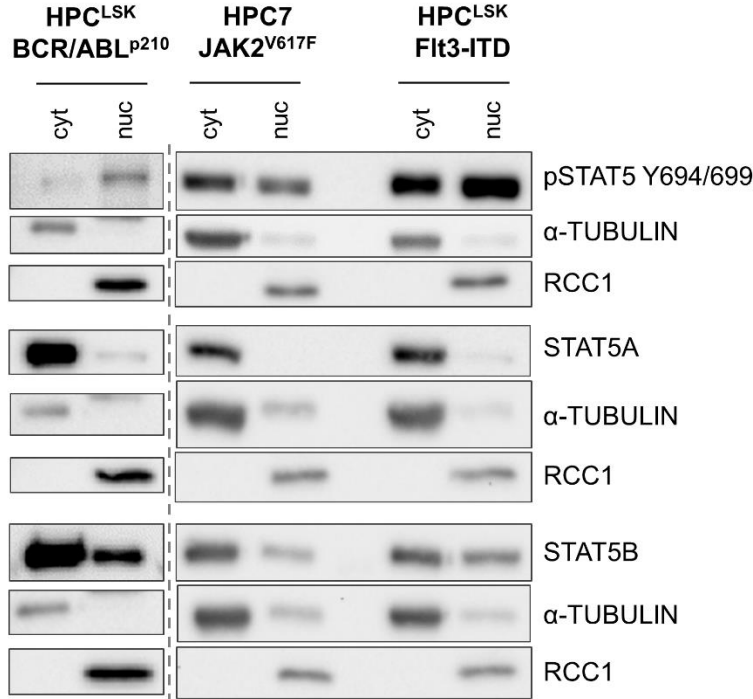
52

Figure S3F



53

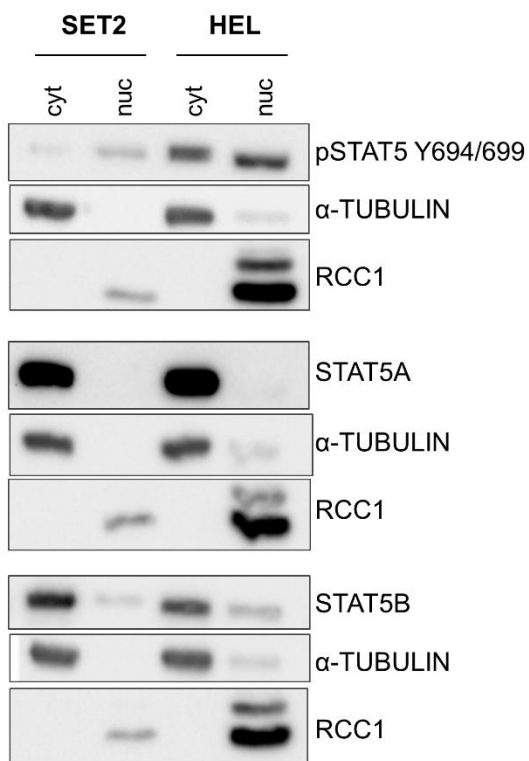
Figure 4C



54

55

Figure S4F

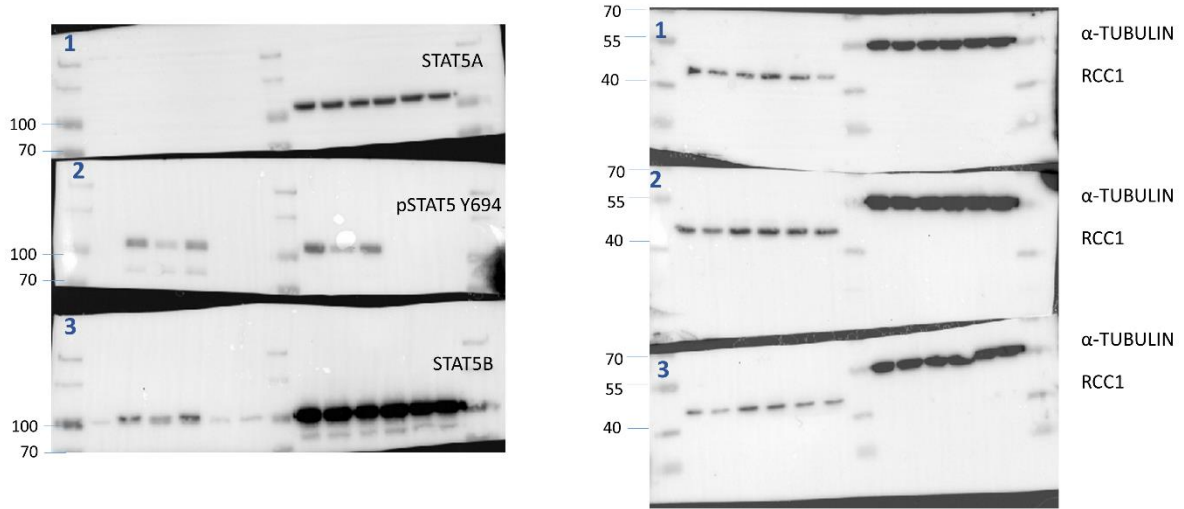


56
57

58 **Part II: Uncropped WB membranes**

Figure 3E

3 8%-polyacrylamide gels have been loaded with the same lysates. The membrane has been cut at the 70 kDa protein ladder signal. The respective loading control for each blot is shown on the right side.



Supplementary Figure 3

3 8%-polyacrylamide gels have been loaded with the same lysates. The membrane has been cut at the 70 kDa protein ladder signal. The respective loading control for each blot is shown on the right side.

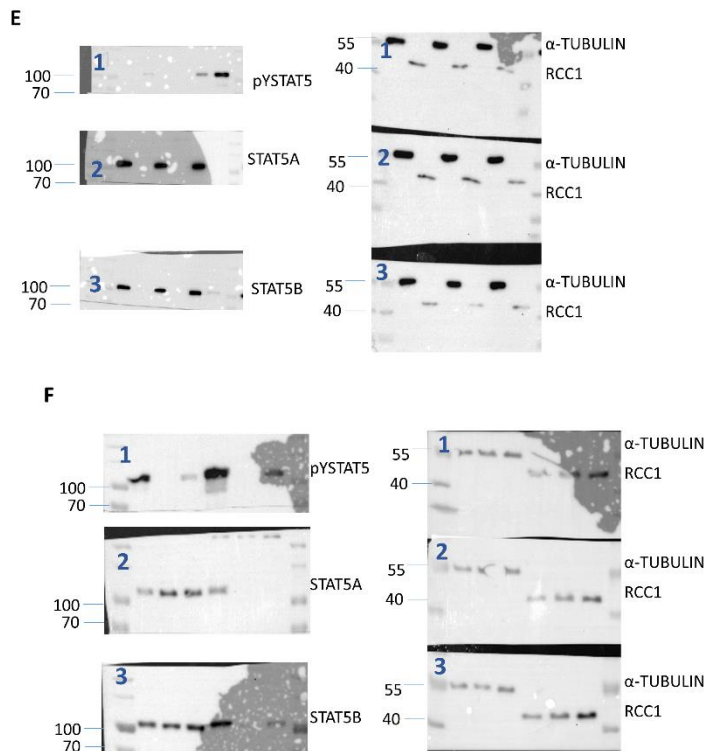
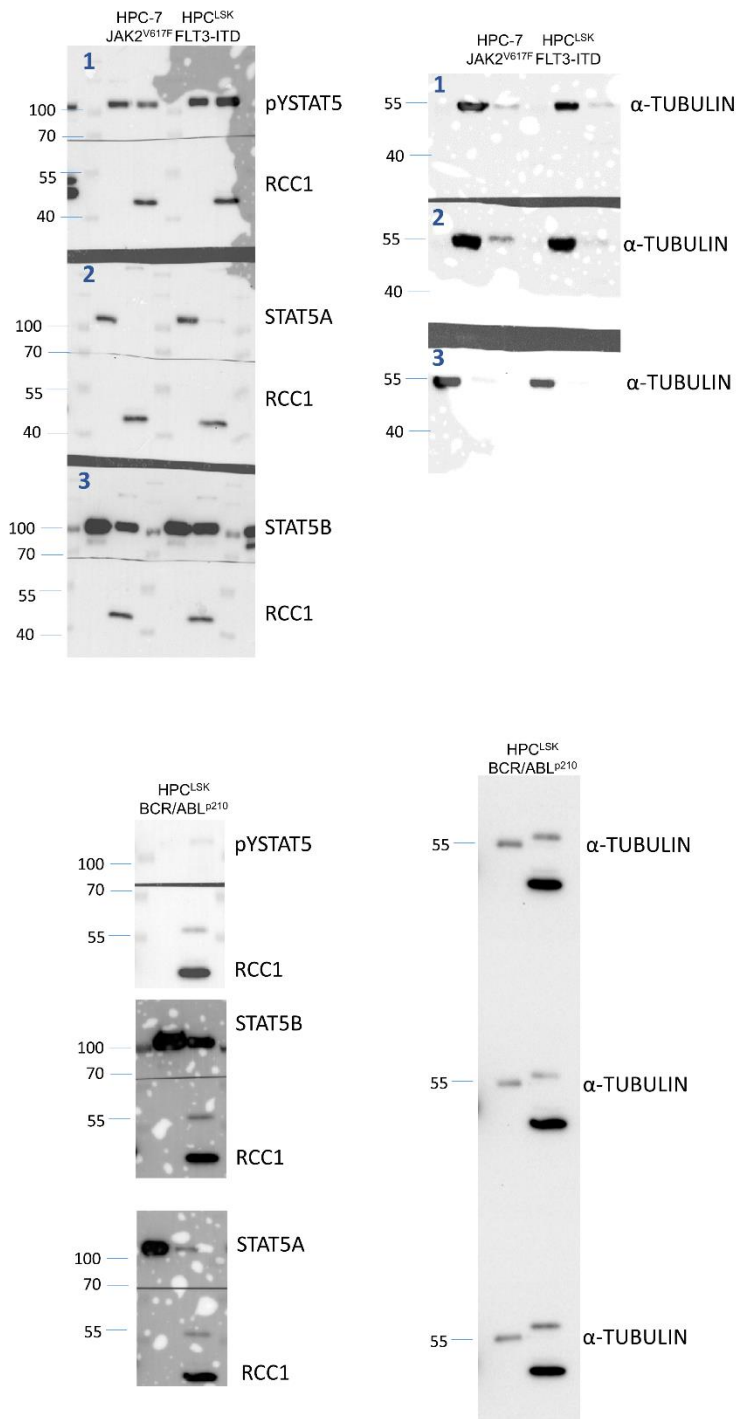


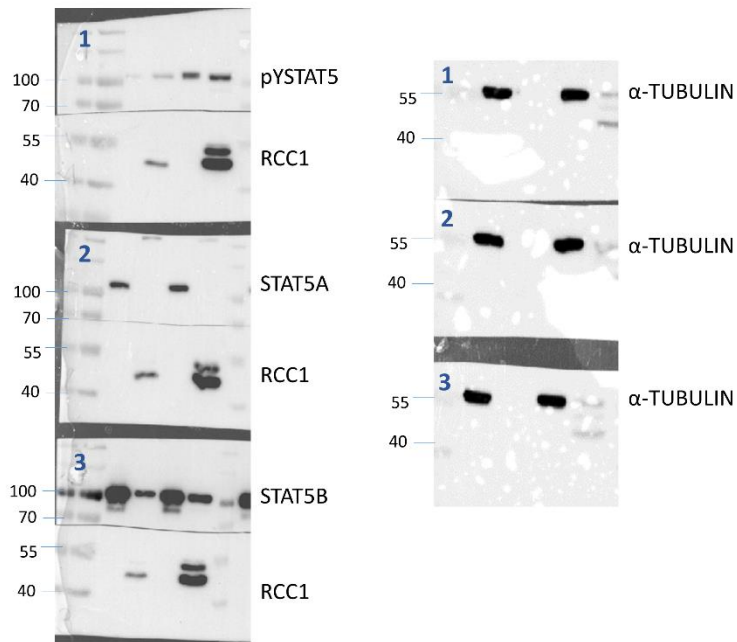
Figure 4C

3 8%-polyacrylamide gels have been loaded with the same lysates. The membrane has been cut at the 70 kDa protein ladder signal. The respective loading controls are shown.



Supplementary Figure 4F

3 8%-polyacrylamide gels have been loaded with the same lysates. The membrane has been cut at the 70 kDa protein ladder signal. The respective loading controls are shown.



61